JPL PUBLICATION 78-64

The Energetic Particle Environment of the Solar Probe Mission

As Estimated by the Participants in the Solar Probe Environment Workshop

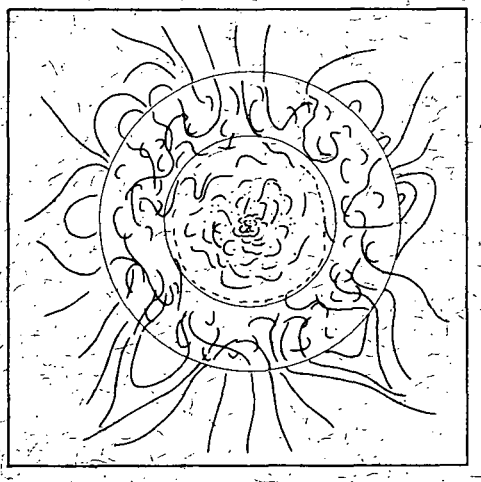

September 1, 1978

National Aeronautics and Space Administration

Jet Propulsion Laboratory
California Institute of Technology
Pasadena, California

JPL PUBLICATION 78-64

The Energetic Particle Environment of the Solar Probe Mission

As Estimated by the Participants in the Solar Probe Environment Workshop

M. Neugebauer
L. A. Fisk
R. E. Gold
R. P. Lin
G. Newkirk
J. A. Simpson
M. A. I. Van Hollebeke

September 1, 1978

National Aeronautics and
Space Administration

Jet Propulsion Laboratory
California Institute of Technology
Pasadena, California

The preparation of this publication was carried out by the Jet Propulsion Laboratory, California Institute of Technology, under NASA Contract No. NAS7-100.

ABSTRACT

NASA's long range plan for the study of solar-terrestrial relations includes a Solar Probe Mission in which a spacecraft is placed in an eccentric orbit with perihelion at four solar radii. In the present concept of the mission, this orbit is attained by a Jupiter gravity-assist maneuver. A reasonable mission plan would require that there be no more than a 1% chance that the peak fluxes and fluences encountered near the Sun exceed those of the Jupiter flyby. It is shown that, if the assumptions in the calculations are correct, this requirement can be met. Some of the crucial assumptions underlying this conclusion are that, at four solar radii, there are no closed, stable configurations in which energetic particles are stored, and that energetic particles do not suffer appreciable energy loss in traveling from 4 solar radii to 1 AU. The spacecraft could suffer fatal radiation damage (1) if it encountered one of the extremely large solar flares which occur, on the average, about once every ten years, (2) if there are invisible regions of trapped radiation and the spacecraft happened to pass through one of them, or (3) if there is some mechanism which causes an adiabatic energy loss so that the near-solar particles are appreciably more energetic than those observed at 1 AU. All these catastrophes are considered to be unlikely. It is also concluded that, although it is highly improbable that solar neutrons would be hazardous to the health of the spacecraft, there is a severe problem in limiting the neutron flux from a radioactive power supply to a level which allows solar neutrons to be detected.

ACKNOWLEDGMENTS

We thank David Chenette of the University of Chicago for his calculation of the near-Sun neutron environment.

Foreword

The Solar Probe Environment Workshop met at the Jet Propulsion Laboratory (JPL) on January 19-20, 1978. The Workshop was convened by M. Neugebauer, JPL. Other authors of the report are L. A. Fisk, University of New Hampshire; R. E. Gold, Applied Physics Laboratory, The Johns Hopkins University; R. P. Lin, Space Sciences Laboratory, University of California, Berkeley; G. Newkirk, High-Altitude Observatory/National Center for Atmospheric Research, Boulder, Colorado; J. A. Simpson, Enrico Fermi Institute, University of Chicago; and M. A. I. Van Hollebeke, Laboratory for High Energy Astrophysics, NASA/Goddard Space Flight Center, and University of Maryland.

CONTENTS

Tables

Figures

I. INTRODUCTION

NASA's long range plan for the study of solar-terrestrial relations includes a Solar Probe Mission in which a spacecraft is sent as close to the Sun as possible. In the present mission concept, the spacecraft components can probably be kept below their maximum operating temperature if the probe does not approach closer than 4 solar radii* (R_s) to the center of the Sun. Figure 1 shows the near-solar portion of the planned trajectory.

The question arises whether or not the energetic particle environment encountered during such a solar flyby with perihelion at 4 R_s might endanger the spacecraft and the mission. The Solar Probe Environment Workshop was formed to consider this problem. The Workshop met at the Jet Propulsion Laboratory on January 19 and 20, 1978. In addition to the authors of this report, the participants were R. W. Davies, T. N. Divine, L. A. Frank, E. F. Koprowski, J. E. Randolph, and E. C. Stone.

Three different methods of placing limits on or estimating the energetic particle flux and fluence during the solar flyby are presented. First, in Section II, photon fluxes observed at 1 AU are used to derive upper limits for the proton and electron fluxes and fluences near the Sun. In Section III, we first use particle observations near 1 AU to estimate the maximum probability that the solar probe will encounter any given level of proton flux and fluence; maximum probabilities are ensured by making a wildly conservative assumption about the distribution of event sizes. We then make best guesses about the relation between the flux observed at 1 AU and the total number of particles released from the Sun and the distribution of event sizes to calculate a best-guess probability that the solar probe will encounter any given level of proton flux and fluence.

Electron and neutron bombardment are discussed in Sections IV and V, respectively. The overall outlook for a mission with perihelion at 4 R_s is discussed in the final Section.

---

* 1 $R_s \approx 0.005$ AU $\approx 7 \times 10^5$ km

II. UPPER LIMITS ON ENERGETIC PARTICLE FLUXES AT THE SUN FROM PHOTON OBSERVATIONS

Energetic electrons and ions produce bremsstrahlung x-ray emission and nuclear gamma-ray line emission, respectively, through collisions with the solar atmosphere. The electrons also interact with the ambient plasma and magnetic field to produce radio emission. Although the mechanisms for coronal radio emission are not quantitatively well understood, ground-based and satellite observations can provide information on the location and extent of the energetic particle populations to distances of many solar radii (Fainberg and Stone, 1974). Observations of the x- and gamma-ray emission can provide quantitative estimates of the spectrum and fluxes of energetic particles in the emission region. These estimates can be used to obtain essentially model-independent upper limits to the energetic proton and electron fluences for the Solar Probe Mission.

Following Lin (1974), consider a volume, V, containing ambient plasma and energetic particles. Let

E	= kinetic energy of an energetic particle with velocity v
$h\nu$	= energy of photon
n_H	= number density of the hydrogen nuclei
$dn(E)/dE$	= density of energetic particles ($cm^{-3}keV^{-1}$)
$d\sigma(E,h\nu)/d(h\nu)$	= differential cross section for photon production ($cm^2 ion^{-1} keV^{-1}$).

Then the photon flux at 1 AU, assuming the particles are isotropic, is

$$\frac{dJ(h\nu)}{d(h\nu)} = \frac{n_H V}{4\pi R^2} \int_{h\nu}^{\infty} v \frac{d\sigma}{d(h\nu)} \frac{dn}{dE} dE \qquad (1)$$

where R = 1 AU = 1.5×10^{13} cm. For non-relativistic electrons the Bethe-Heitler cross-section is applicable

$$\frac{d\sigma(E,h\nu)}{d(h\nu)} \approx 1.58 \times 10^{-24} \frac{1}{Eh\nu} \times \ln\left[\left(\frac{E}{h\nu}\right)^{1/2} + \left(\frac{E}{h\nu} - 1\right)^{1/2}\right] cm^2 ion^{-1} keV^{-1} \qquad (2)$$

Equation (1) can be inverted with (2) to obtain the electron spectrum. For a power law x-ray spectrum

$$dJ/d(h\nu) = A(h\nu)^{-\gamma} \tag{3}$$

we obtain

$$\frac{dJ_e}{dE} = \frac{vdn}{dE} = 2.27 \times 10^{51}\gamma(\gamma-1)^2 B(\gamma-\tfrac{1}{2},3/2)\frac{AE^{-\gamma+1}}{n_H V} \tag{4}$$

where $B(x,y)$ is the beta function.

The strongest solar γ-ray line, both from theory (Ramaty et al., 1975) and observation (Chupp et al., 1973), is located at 2.22 MeV. This line results from neutron capture by hydrogen and the subsequent deexcitation of the deuterium. The neutrons are produced by energetic protons and heavier ions interacting with various nuclei. Detailed calculations have been performed on the neutron production and propagation to obtain the 2.22 MeV photon yield (Wang and Ramaty, 1974). For typical power law proton spectra with exponents of -2 to -3, the 2.22 MeV flux at 1 AU is given by

$$J_{2.2}(\text{photons cm}^{-2}\text{sec}^{-1}) \approx 5 \times 10^{-46} n_p(>10 \text{ MeV}) n_H V \tag{5}$$

Thus

$$J_p(>10 \text{ MeV})(\text{cm}^2\text{sec})^{-1} \approx n_p v \approx \frac{10^{55}}{n_H V} J_{2.2} \tag{6}$$

It is important to note that these relationships hold at a given instant of time. That is, the instantaneous number and spectrum of energetic protons or electrons in the region is related to the instantaneous gamma-ray or x-ray emission.

Most of the x-ray and γ-ray emission probably originates from regions much closer to the Sun than the solar probe will traverse. An absolute upper limit to the energetic particle fluxes would thus be obtained under the assumption that all the emission comes from the 4 to 10 R_s region. The density n_H estimated from radio observations (Fainberg and Stone, 1974) is $\sim 3 \times 10^4 \text{cm}^{-3}$ at 10 R_s and $\sim 3 \times 10^5 \text{cm}^{-3}$ at 4 R_s. We

assume the particles fill a region ∿1 steradian wide and ∿2 R_s thick at 4 R_s (total volume $\sim 10^{34}$ cm^3) and that the volume at other distances scales as r^3. Then $n_H V \gtrsim 4 \times 10^{39}$, approximately constant from 4 to 10 R_s. Taking the observed x-ray and γ-ray emission (or upper limits) for quiet, one-a-day flares, and very large flares, and using equation (4) and (6), we have computed the maximum particle fluxes at 4 to 10 R_s distances (Table 1). The total integrated particle fluences depend on the flare emission period, $\Delta t \gtrsim 10^2$-10^3 sec. For non-flare fluxes, $\Delta t \gtrsim 10^4$ sec, the traversal time across 1 steradian solid angle.

These flux and fluence limits are quite high, but more sensitive observations with better x-ray and γ-ray instruments over the next few years can substantially reduce these limits.

TABLE 1. UPPER LIMITS ON ENERGETIC PROTONS AND ELECTRONS FOR SOLAR PROBE

	Quiet-time (non-flare)	Typical flare	Very large flare
I. Energetic protons			
2.22 MeV photon flux* $(cm^2 sec)^{-1}$	$<5\times10^{-3}$	$<5\times10^{-3}$	∿0.3
>10 MeV proton flux $(cm^2 sec)^{-1}$	$<10^{13}$	$<10^{13}$	$<10^{15}$
>10 MeV proton fluence cm^{-2}	$<10^{17}$ ($\Delta t = 10^4$ sec)	$<10^{16}$ ($\Delta t = 10^3$ sec)	$<10^{18}$ ($\Delta t = 10^3$ sec)
II. Energetic electrons			
X-ray parameters** $\frac{dJ}{d(h\nu)} = A(h\nu)^{-\gamma}$ A	<20	$\sim 5\times10^5$	$\sim 1\times10^6$
γ	∿2	∿4.5	∿2.7
>20 keV electron flux $(cm^2\ sec)^{-1}$	$<2\times10^{13}$	$<3\times10^{14}$	$<2\times10^{17}$
>1 MeV electron flux $(cm^2\ sec)^{-1}$	---	$<2\times10^{10}$	$<10^{14}$
>20 keV electron fluence (cm^{-2})	$<2\times10^{17}$ ($\Delta t = 10^4$ sec)	$<3\times10^{16}$ ($\Delta t = 10^2$ sec)	$<2\times10^{20}$ ($\Delta t = 10^3$ sec)
>1 MeV electron fluence (cm^{-2})	---	$<2\times10^{12}$	$<10^{17}$

*From Chupp et al. (1968) and Chupp et al. (1973).

**From Datlowe et al. (1974), Lin and Hudson (1976), and Kane (1978).

III. PROTON FLUXES ESTIMATED FROM PROTON OBSERVATIONS

A. ASSUMPTIONS

Protons and electrons are the most abundant solar energetic particles detected in interplanetary space and are the most likely to be observed at a few solar radii.

At 1 AU, the observed solar particle peak intensity ranges from greater than 10^3 particles/cm^2-sec-ster at energies above 20 MeV down to micro events with integral intensity above 20 MeV some five orders of magnitude lower. The energies of particles range from tens of keV up to some 20 GeV in the infrequent high energy solar particle events.

Below 20 MeV, a variety of different types of proton events has been observed, such as flare associated particle events, corotating particle streams and energetic storm particle events in addition to a small galactic component. The origin of many of these event types is now becoming well understood. The flare associated events have a well defined solar signature starting with an active region, radio and x-ray emission, and a solar flare. In the case of the corotating streams of energetic particles which represent the dominant component observed during solar minimum, there is strong evidence of a positive gradient between 0.3 AU and 3-5 AU (McDonald et al., 1976; Shea and Smart, 1973; Simnett, 1972; Van Hollebeke et al., 1975; and Van Hollebeke et al., 1978) which indicates that acceleration is taking place in the interplanetary medium. For those events, it is therefore expected that the intensity of low energy particles will be smaller near the Sun than in interplanetary space (typically $\lesssim$ 10 particle/cm^2-sec-sr-MeV at 1 MeV at 1 AU with an exponential momentum spectrum of the form $dJ/dP \propto \exp(-P/P_o)$ with P_o = 9-15 MV and thus of small importance compared to the intensity of flare associated particle events.

Since the observations of protons below 20 MeV are greatly influenced by interplanetary propagation effects (acceleration, as indicated above, deceleration, diffusion, shock effect, etc.), it is not easy to infer the solar condition at those energies from interplanetary observations.

However, at higher energy, these interplanetary effects are less important, thus making possible the use of proton observations above

20 MeV to define energetic particle conditions at the Sun. Note also that since the range of a 20 MeV proton is $\sim$0.5 g/cm^2 or 0.2 cm in aluminum (it is ten times smaller at 5 MeV), this energy range is also the most relevant one in defining the expected radiation environment which could be hazardous to a spacecraft with perihelion between 2 and 10 solar radii. However, if needed, the conclusion drawn from proton observations above 20 MeV can be extrapolated to low energy.

In estimating the probabilities of encountering different levels of radiation, we make three basic assumptions:

i) We assume that there are no permanent storage configurations at altitudes as great as 4 solar radii. The evidence that stable closed loops in the corona do not extend beyond 2.5 R_s is rather extensive. Observations of the eclipsed Sun allow the density structure of the corona to be established out to about 4 or 5 R_s. Assuming the density structure to outline the coarse configuration of the field, we note that reviews (Newkirk, 1967) of such observations covering a century of eclipses set the upper limit of stable closed coronal forms at $R \simeq 2.5\ R_s$. Infrared and satellite observations out to $13R_\odot$ confirm this conclusion (Tousey et al., 1974). Theoretical calculations of the interaction of coronal magnetic fields and the expanding solar wind plasma have grown quite sophisticated in the last decade (see Pneuman, 1968 and 1973) and reach the same conclusion. Above $\sim$2.5 R_s the dynamic forces of the solar wind are sufficient to open up the magnetic field into interplanetary space.

Some investigators argue that invisible, closed, stable magnetic loops (ICSML) may still exist above the canonical 2.5 R_s. Although caution must always be exercised in confronting the invisible, the proponents of such ICSML's have thus far failed to answer:

- How do ICSML's avoid containing material and thus evade detection while other quite substantial coronal structures are well documented in the region 2.5 - 13 R_s?
- How do ICSML's avoid being swept out by the solar wind?
- What phenomena indicate their existence?

ii) We assume that at a given radial distance above 4 R_s the total number of particles at a given energy, crossing unit area during a sufficiently long time, is the same at all solar latitudes and longitudes. Flare events occur at many different locations on the Sun, and energetic particles can propagate through the corona many tens of degrees in longitude and also presumably in latitude. At least within solar-active zones(e.g., <30° in latitude) the total number of emitted particles should thus be spread evenly in longitude and latitude. However, this assumption may cause us to overestimate the fluences at high solar latitudes, which are far from active regions.

iii) We assume that energetic particles propagating from 4 R_s to 1 AU do not suffer appreciable energy loss; i.e., a 20 MeV proton observed at Earth was a 20 MeV proton at 4 R_s. Any energy loss would result principally from adiabatic deceleration in the expanding solar wind. However, particle mean-free paths in the interplanetary medium appear to be too large for this to be a major effect, except perhaps during the decay with time, at late times during flare events.

B. MAXIMUM PROBABLE PROTON FLUX AND FLUENCE

According to Reedy (1977), in the eight years between 1965 and 1973 the total fluence at Earth of solar protons with energy $\geq$ 20 MeV was 3×10^9 cm^{-2}, which corresponds to an average flux $I_{avg} = 12$ cm^{-2} s^{-1}. If the flux were organized into discrete events, each with intensity I, then an event would be in progress a fraction I_{avg}/I of the time. Since the maximum probability of observing a given flux level I would correspond to the assumption that all of the solar events during this 8 year period had this same intensity I, we find that

$$P_{max}(I) \text{ at 1 AU} = I_{avg}/I.$$

If we further assume that the solid angle of the event is independent of distance from the Sun, then $P_{max}(I)$ would vary as the inverse square of the solar distance, and, at 4 solar radii,

$$P_{max}(I) = \frac{I_{avg}}{I}\left(\frac{4\ R_s}{1\ AU}\right)^2 = \frac{3 \times 10^4}{I} \qquad (7)$$

for protons above 20 MeV, where I is in units of protons cm^{-2} s^{-1}.

Clearly, (7) is a simple result. It yields, for example, that there is a maximum of a 1% chance that in a given region near 4 R_s the spacecraft will encounter a flux of 3×10^6 protons/cm^2-sec, with energies $\geq$20 MeV. Since this result holds for any region near 4 R_s through which the spacecraft passes, there is also a maximum probability of 1% that it will encounter a fluence of It_{sp}, where t_{sp} is the time spent by the spacecraft near perihelion. With $t_{sp} \tilde{\sim} 16$ hours, this fluence is $\sim 2 \times 10^{11}$ protons/cm^2.

C. MOST LIKELY PROTON FLUX AND FLUENCE

We next attempt to calculate a more realistic probability of encountering given proton fluxes and fluences by inferring the total number and energy spectrum of particles released at the Sun in each event as well as the probable frequency of events of different sizes. Because of the many assumptions and extrapolations made, the resulting probabilities may be less reliable than the upper limits and maximum probabilities calculated in the two previous Sections.

1. TOTAL NUMBER OF PARTICLES INJECTED AS A FUNCTION OF OBSERVED PEAK FLUX

There are several methods of estimating the total number of particles released into the interplanetary medium during a solar flare event. We first make the assumption that we are only interested in particles that reach $\sim$1 AU (i.e., we assume that essentially all particles that propagate out to perihelion of the Solar Probe orbit will eventually reach 1 AU without significant energy loss). Then two methods of estimating the total particle injection are attractive. Spherically symmetric diffusion models with impulsive injection give a simple result for the total number of particles that depends only on the peak flux and the radius at which it is observed. However, this method is model dependent and the specific assumptions of impulsive injection and spherical symmetry are in direct contradiction to observations.

Another technique for estimating the total particle injection can be constructed from the continuity equation. Essentially, the net energetic particle streaming along the flux tube of the spacecraft may be computed from the observed flux and anisotropy measurements. The

net streaming need just be summed throughout the event to determine the total number of particles escaping through the flux tube. This technique has the advantage that it is independent of any model of interplanetary energetic particle propagation and relies purely on observed quantities. However, there are difficulties in implementing this technique since it requires much more data than just the peak flux which is all that is needed by the spherically symmetric diffusive approximation with impulsive injection. For the net streaming technique both the flux and the first harmonic of the Fourier decomposition of the anisotropy must be known as a function of time throughout the event with sufficiently fine time resolution and statistical accuracy to define the outward current. Unfortunately, there have been very few detectors with angular sectoring and sufficient geometric factors and duty cycle to make statistically significant anisotropy measurements in the 20 MeV range; existing measurements primarily cover only a few of the larger events during the latter part of solar cycle 20. However, high quality measurements of 20 MeV proton time histories are available during most of the solar cycle. We show below that the particle streaming in the flux tube of the spacecraft may be estimated to within about a factor of 2 purely from the flux time history thereby removing the major problem with the implementation of this technique. But first we shall apply both the diffusion model and the streaming technique to a sample solar particle event.

a. APPLICATION OF THE BASIC TECHNIQUES

We shall apply both the diffusion model and the streaming technique to the October 30, 1972, solar particle event. This event has been chosen because of the availability of anisotropy data from IMP-7. It is one of the largest events during solar cycle 20 and is also one in which the time histories at >10 MeV look "classical" and therefore the two methods might be expected to yield similar results. However, the time span of interplanetary particle injection at lower energies was quite extended during this event and if there was also an extended injection at >20 MeV, it could contribute significant disagreement between the two methods.

The data are from the 25.2 - 49.5 MeV proton channel of the APL/JHU experiment on IMP-7 which has 8 angular sectors in the ecliptic plane.

Three hour averages of the differential flux at 37.3 MeV and the first harmonic of the angular distribution are listed in Table 2 for the period when the flux was greater than 10^{-3} $(cm^2$ sec sr MeV$)^{-1}$ which is within about two orders of magnitude of the peak flux. Let us now look at the total particle release estimates for an observer at 1 AU.

i. SPHERICALLY SYMMETRIC DIFFUSION MODEL WITH IMPULSIVE INJECTION

The diffusion model gives the simple result

$$N = \frac{8 J_m r^3}{v} \left(\frac{6}{\pi e}\right)^{-3/2} \tag{8}$$

where N is the total number of particles/MeV, J_m is the maximum observed differential flux, r is the distance from the sun and v is the particle velocity. At 1 AU this reduces to

$$N = J_m \times 5.3 \times 10^{30}.$$

Substituting the peak flux from Table 2

$$N = 5.1 \times 10^{29} \text{ MeV}^{-1}.$$

TABLE 2. FLUX AND ANISOTROPY DURING THE OCTOBER 30, 1972 EVENT

DAY	HOUR	25.2-49.5 MeV FLUX (10^{-3})	ANISOTROPY MAGNITUDE
304	9-11	6.1	.92
	12-14	11	.26
	15-17	17	.38
	18-20	28	.21
	21-23	48	.17
305	0-2	85	.36
	3-5	57	.34
	6-8	28	.16
	9-11	16	.17
	12-14	11	.13
	15-17	5.4	.25
	18-20	1.6	.42

Peak flux 9.7×10^{-2} $cm^{-2}s^{-1}sr^{-1}MeV^{-1}$ at 0100-0200 on October 31.

ii. OBSERVED STREAMING

If energy changes are insignificant, the total number of particles flowing out along a flux tube during a flare event is

$$N = \int_0^\infty dt \int_A \vec{S} \cdot d\vec{A}$$

where $\vec{S}$ is the net particle flux and A is the area of the flux tube.

Early in the event, when the anisotropies are large and field aligned, the volume being considered is truly a flux tube and $S \simeq S_{||}$. The net current is essentially the measured anisotropy as long as the magnetic field vector is close to the ecliptic plane. Starting near the peak of the event, when the anisotropies usually cease to be strongly field aligned, the radial component of the observed anisotropy may be taken as a good approximation to the particle loss.

Let us now apply this technique to the October 1972 event assuming spherical symmetry so that the result may easily be compared with the diffusive model calculation above. Then

$$N = 4\pi \ (1 \text{ AU})^2 \sum_i J_i \xi_i \tau_i \qquad (9)$$

where J_i is the observed flux during the ith time period τ_i, and ξ_i is the effective outward streaming anisotropy. Using the observed 3-hr anisotropy amplitudes for ξ_i we get

$$N = 2.7 \times 10^{30} \text{ MeV}^{-1}.$$

This is a factor of $\sim$5 greater than the estimated total particle release from the spherically-symmetric, impulsive-injection diffusion model. Since this calculation has also assumed spherical symmetry, it's the impulsive injection assumption in the diffusive model that has probably contributed the greatest source of error.

b. ANGULAR DISTRIBUTIONS

Clearly spherical symmetry is not what is observed; however, there have been very few observations of the angular dependence of solar particle events. The cleanest observation reported has been the April 10, 1969, event which was observed by 5 spacecraft covering more than 180° of heliographic longitude (Gold et al., 1977a). The intensity of $\gtrsim$ 10 MeV protons during this event was found to fall off exponentially from the center of a preferred release zone with an e-folding angle for these azimuthal gradients of $\sim$25°. The center of the distribution during this event, however, was $\sim$100° west of the flare site. Statistical studies of the peak flux during an event as a function of the angular distance to the flare site have been presented by McKibben (1972), Reinhard (1975), and Van Hollebeke et al. (1975). They confirm the existence of azimuthal gradients. However corotation, possible displacements of the distribution center from the flare site, etc., preclude accurate estimates of the gradients from statistical studies. If we use the distribution of peak fluxes for events associated with flares from 20-60° west and 20-60° east solar longitude, as reported by Van Hollebeke et al., we derive an estimate of e-folding angles of 25 to 70°. McKibben's observations of the May 1968 event by IMP-4, Pioneer 6, and Pioneer 7 lead to e-folding angles of 30-50° at $\sim$15 MeV. Gold et al. (1977b) and Roelof et al. (1975) have examined the azimuthal gradients in individual events by solar wind mapping techniques. They found e-folding angles ranging from 10 to 30° with an average near 20° that were approximately energy independent; however their work was in the 0.3-5 MeV range and the gradients may not have the same values at $\gtrsim$ 20 MeV.

In spite of the limited direct evidence, we shall assume that all solar particle events in the $\gtrsim$ 20 MeV range have azimuthal gradients with e-folding lengths of $\sim$20-30°. Then, normalizing to the center of the distribution, the ratio of the total number of particles injected into the interplanetary medium in a distribution with e-folding angle θ_o to the total injection in the spherically symmetric distribution is

$$\frac{N(\theta_o)}{N_{(spherical)}} = \frac{1+ \exp(-\pi/\theta_o)}{2\ (1 + 1/\theta_o^2)}$$

where θ_o is the e-folding angle. Thus, with gradients, the total injections are only $\sim$0.05 to 0.1 of the spherically symmetric estimates. For the example above, applying the observed streaming technique to the October 1972 event, an azimuthal gradient with an e-folding length of 30° would, if the Earth were at the center of the distribution, reduce the estimate of the total injection to

$$N = 3 \times 10^{29}\ MeV^{-1}$$

Since we are not certain that the Earth was exactly at the center of the distribution, we will assume that $N = 4 \times 10^{29}\ MeV^{-1}$ for the October 1972 event, for which the peak flux was $10^{-1}\ cm^{-2}s^{-1}sr^{-1}MeV^{-1}$. If we follow Equations (8) and (9), assume that the total number of particles injected is proportional to the peak flux, and use the October 1972 event for normalization, we obtain

$$N = 4 \times 10^{30}\ J_m \qquad (10)$$

for J_m in units of $cm^{-2}s^{-1}sr^{-1}MeV^{-1}$ and N in units of MeV^{-1}.

c. PROTON ENERGY SPECTRA

The value of N calculated above is the total number of particles injected per MeV. To calculate N_o, the total number of particles above 20 MeV, we must make some assumptions about the proton energy spectrum.

The energy spectra observed at 1 AU represent the combined effects of the source spectrum, coronal transport, the release into the interplanetary medium, and interplanetary diffusion and velocity dispersion. It has been shown that in measuring the particle spectrum near the maximum particle intensity, interplanetary effects are minimized. This spectrum is then representative of the energy spectral distribution both close to the Sun and after release into the interplanetary medium (Van Hollebeke et al., 1975).

Based on observations of some 100 solar flare-associated particle events detected at 1 AU, it was found that for protons in the energy range 20-80 MeV, a power law in differential kinetic energy of the form $J \propto E^{-\gamma}$ appears to give the best representation. Figure 2 shows a representative sample of spectra. The spectral index γ varies with the flare longitude relative to the observer from $\gamma = 2$ to $\gamma = 5.5$ as shown in Figure 3. It has been argued that for heliolongitude 20-80° west of the Earth's central meridian (preferred connection region for an observer near Earth) the spectral index γ is representative of the source spectrum. For these heliolongitudes, γ displays a surprisingly small range, varying between 2.0 and 3.2 and a mean of 2.7. The steepening of the spectra with increasing angular separation from the preferred connection region can be explained in terms of an energy or velocity dependent particle escape rate from the corona.

It is therefore expected that at any given point outside the escape boundary into the interplanetary medium, the spectral distribution of the particles will be dependent on the observer's position relative to the flare site: near the flare site, the particle population will display the characteristic source spectrum:

$$J \propto E^{-2.7 \pm 0.5} \tag{11}$$

while away from the flare, the spectrum will be poor in energetic particles as those will have escaped faster (thus, a steep spectrum). From the point of view of modeling the expected particle environmental condition at a few solar radii, it is reasonable to assume an average spectrum equal to that of the characteristic source spectrum.

N, the total injection per MeV, was determined above from measurements over the energy range 25.2 to 49.5 MeV. Equation (11) can be used to convert N to N_o as follows:

$$N_o = (49.5 - 25.2)\, N \int_{20}^{\infty} E^{-2.7}\, dE \Big/ \int_{25.2}^{49.5} E^{-2.7}\, dE = 53\, N$$

or,

$$N_o = 2 \times 10^{32}\, J_m. \tag{12}$$

2. FREQUENCY OF EVENTS VERSUS PEAK FLUX

a. ENERGETIC SOLAR PARTICLE EVENT PROBABILITY

The frequency of particle events produced at the Sun can be readily deduced from the nearly continuous interplanetary observations made with Earth orbiting satellites at 1 AU during solar cycle 20 (1964-1976). Figure 4 shows the number of > 20 MeV proton events with peak intensity > 0.5 protons/cm^2-sec-ster detected at 1 AU between 1962 and 1975. Also shown in the figure is the number of sea level neutron monitor events (with energy > 500 MeV/nucleon) from 1956 to 1972 (Shea and Smart, 1973; McDonald, Fichtel and Fisk, 1974). The solar cycle dependence of event frequency can be easily appreciated for > 20 MeV proton events, using the Zurich sunspot number as a simple index to indicate the overall level of solar activity. For solar cycle 20 (which represents a good approximation of the mean solar activity between solar cycle 8 and 20, as indicated in Solar Geophysical Data, 1977) there is a linear relation between the number of events observed per year and the yearly-averaged sunspot number as shown in Figure 5. In this figure, the error bars attached to the number of events represent a 1σ statistical fluctuation.

Note that the number of events/year represents all the > 20 MeV proton events with peak intensity > 0.5 protons/cm^2-sec-ster detected by Earth orbiting satellites during every year from 1964 through 1975. Assuming that the event visibility conditions are the same at a few solar radii as at 1 AU, the event frequency seen by a solar probe during perihelion passage should be the same as that indicated in Figure 5. The event visibility at 1 AU has been interpreted in terms of coronal transport and release into interplanetary space. It is therefore expected that the event frequency outside the corona (> 3 R_s, below which coronal transport may take place) will be the same as at 1 AU.

The equation of the straight line through the data in Figure 5 is:

$$\text{Number of events per year} = 0.15\ R_Z - 0.60$$

where R_Z is sunspot number. The probability of an event occurring in any hour is thus given by

$$P(>0.5\ \text{cm}^{-2}\text{s}^{-1}\text{sr}^{-1}\text{MeV}^{-1}) = (1.7\ R_Z - 6.8) \times 10^{-5}. \qquad (13)$$

b. SIZE DISTRIBUTION OF FLARE ASSOCIATED PARTICLE EVENTS

The energetic solar particle event frequency is not only a function of time but it is also a function of intensity and energy. The number of events per unit intensity as a function of intensity is displayed in Figure 6 for all the events detected by the GSFC cosmic-ray experiments on the Earth orbiting satellites IMP 4 and IMP 5 between 1967 and 1972 (Van Hollebeke et al., 1975). To minimize the effect of the spectral dependence upon longitude, the peak proton intensity measured at 40 MeV is used to characterize the size of the event. The galactic background observed at 1 AU fixes the lower limit of detectability of event intensity to $\sim 10^{-4}$ particles $cm^{-2}s^{-1}sr^{-1}MeV^{-1}$ above 20 MeV. The size distribution of all detected particles can be adequately described by $d\eta/dJ \propto J_m^{-\alpha}$ where J_m is again the maximum differential intensity at 1 AU, in units of particle $cm^{-2}s^{-1}ster^{-1}MeV^{-1}$ and $d\eta$ is the number of events in the range of intensity dJ. α is found to be 1.15 ± 0.05. The size distribution of the flare-identified events is also plotted in this figure. Note that the form of the distribution is the same for the flare-identified events and for the total number of events. It is also found that the form of the distribution is independent of the observer's position relative to the associated flare except that the number of events per unit of intensity decreases by a factor ~ 2 when the observer's position relative to the associated flare is > 80° away from the best connection region. Note that in Figure 5, the number of events per year for > 20 MeV proton with peak intensity > 0.5 protons/cm^2s sr is the fraction per year of the integral above $\sim 6 \times 10^{-3}$ protons/cm^2-sec-sr-MeV obtained from Figure 6 assuming $J \propto E^{-2.7}$.

When we combine this result with Equation (13) we find that the probability of observing a peak flux $\geq J_o$ in any one hour is given by

$$P(\geq J_o) = (1.7\ R_Z - 6.8) \times 10^{-5} \left\{ \int_{J_o}^{\infty} \frac{d\eta}{dJ}\, dJ \Big/ \int_{6\times10^{-3}}^{\infty} \frac{d\eta}{dJ}\, dJ = \left(\frac{6 \times 10^{-3}}{J_o} \right)^{0.15} \right\}$$

The hourly probability of the injection of $\geq N_o$ particles can then be found from Equation (12):

$$P(\geq N_o) = (0.55\ R_Z - 2.2)\ N_o^{-0.15} \qquad (14)$$

3. EXPECTED PROTON FLUX AND FLUENCE

We are concerned with the encounter of the Solar Probe with energetic particles, particularly as they influence the two parameters:

$$I = \int_{\Omega}\int_{E_0}^{\infty} J(\theta,\phi)\ d\omega\ dE$$ = the mean intensity above some cut-off energy ($E_0 \sim 20$ MeV for protons)

and

$$F = \int_{t_0}^{\infty} I\ dt$$ = the fluence of such particles

During its perihelion passage at 4 R_s the Probe will spend $\sim$ 16 hrs (5.8×10^4 sec) in the region $R < 10\ R_s$ and <u>may</u> encounter energetic particles of several distinct populations:

(1) Particles escaping on open field lines on their way into interplanetary space,

(2) Particles stored in stable closed magnetic configurations, and

(3) Particles temporarily resident in closed, rapidly evolving magnetic configurations.

The distinction between the three cases will be examined below. Throughout we shall attempt to define the probability that a specific event will befall the Probe during its 16 hours of passage below 10 R_s. The following illustration is useful.

From the last subsection, we know $P(N_o)$, the probability that in any given hour an event will occur with a total particle output N_o above $\sim$ 20 MeV for protons. The probability that during 16 hours <u>at least one</u> such event will occur is

$$P'(N_o) = 1 - (1 - [P(N_o)]^t), \text{ where } t = 16$$

and for $P(N_o) << 1$

$$P'(N_o) = 1 - 1 + tP(N_o) + \ldots \approx tP(N_o)$$

a. CASE (a) (IMMEDIATE ESCAPE)

At a distance R we have the approximation

$$I_a \sim \frac{N_o}{\omega R^2 \tau},$$

where ω = solid angle of the escape region as seen from the center of the Sun

τ = event duration.

Also

$$F_a \sim I_a \frac{\ell}{v_{sc}}$$

where

ℓ = length of spacecraft trajectory in the region ω

v_{sc} = spacecraft speed.

The probability of the spacecraft's encountering such an event in any hour is

$$P(I_a) \simeq \frac{\omega}{4\pi} P(N_o)$$

and that at least one such event be encountered during perihelion passage is

$$P'(I_a) \simeq t(\text{hrs}) \frac{\omega}{4\pi} P(N_o)$$

If we take $\omega = 1$ sr, $R = 8\ R_s = 5.6 \times 10^{11}$ cm, $t = 16$ hr $= 5.8 \times 10^4$ s, and $v_{sc} = 3 \times 10^7$ cm s^{-1}, then

$$I_a = 5.5 \times 10^{-29}\ N_o\ cm^{-2}\ s^{-1} \tag{15}$$

$$F_a = 1.0 \times 10^{-24}\ N_o\ cm^{-2} \tag{16}$$

$$P' = \frac{16}{4\pi} P(N_o) = 1.27\ (0.55\ R_Z - 2.2)\ N_o^{-0.15}$$

The probabilities P' of encountering flux levels I_a and fluences F_a due to immediate escape for years in which $R_Z = 100$ and 200 are plotted in Figures 7 and 8 together with the maximum probabilities calculated in Section IIIB.

b. CASE (b) (STABLE CLOSED LOOPS)

As discussed in Section IIIA, we believe that there are no stable closed loops which extend to 4 R_s. Therefore $P'(I_b) = 0$.

c. CASE (c) (CORONAL TRANSIENTS)

For this case we assume that all particles which escape are instantaneously injected into a volume V_{trans}. Then for an isotropic particle distribution

$$I_c \simeq \frac{1}{3} \frac{N_o v}{V_{trans}}$$

and

$$F_c \simeq I_c \frac{\ell}{v_{sc}}$$

where v is the particle speed. For the probability, we take

$$P(I_c) = P_T\ \phi(N_o)\ \frac{\omega}{4\pi} \tag{17}$$

where P_T is the probability of a transient event anywhere on the Sun during any hour, $\phi(N_o)$ is the fraction of transients with particle

output $\geq N_o$, and ω is the solid angle subtended by an approximately radial transient. To estimate $P_T \, \emptyset(N_o)$, we can either assume (i) that the only transients which contain energetic protons ($\geq$ 20 MeV) are those for which energetic particles are detected at 1 AU, in which case

$$P_T \emptyset(N_o) = P(N_o) \tag{18}$$

where $P(N_o)$ is given by Equation (14), or (ii) that most transients contain energetic particles which do not reach 1 AU. Since transients have not been observed to return to the Sun (Gosling et al., 1974) and a large fraction of particles injected into interplanetary space should eventually be detected, we conclude that the second case is unrealistic and that only a small fraction of transients contain energetic particles. We note, however, that since the average rate of coronal transients during 1973 was 0.5 day^{-1} (Hildner et al., 1976), whereas Figure 4 shows 6 energetic proton events in 1973, only 3% of the transients led to a detectable proton event. If all transients do contain energetic particles and the distribution of event sizes is the same as at 1 AU, then we may be underestimating the radiation hazard by a factor of 30; we believe this to be unlikely, however.

From Equations (17) and (18), the probability of at least one encounter with a transient containing energetic particles is

$$P'(I_c) = t(\text{hrs}) \, P(N_o) \, \frac{\omega}{4\pi}$$

For the geometry of the transient we consider two models - that of a "bubble" and that of a single flux "rope." We assume that a bubble occupies a cone of 60° as seen from the center of the Sun and extends from 4 to 10 R_s. Then ω = 0.84 sr and $V_{trans} = 245 \, R_s^3 = 8.3 \times 10^{34}$ cm^3. With $\ell = 8 \, R_s$, $v_{sc} = 3 \times 10^7$ cm s^{-1}, and $v = 10^{10}$ cm s^{-1}, we obtain

$$I_c = 4.0 \times 10^{-26} \, N_o \, cm^{-2} sec^{-1}$$

$$F_c = 7.5 \times 10^{-22} \, N_o \, cm^{-2}$$

$$P'(I_c) = 1.1 \, (0.55 \, R_Z - 2.2) \, N_o^{-0.15}$$

For a rope transient of height h and rope radius a,

$$V_{trans} \sim 3h\ \pi a^2$$

and for

$$h = 10\ R_s$$

$$a = 0.2\ R_s$$

$$V_{trans} = 1.27 \times 10^{33}\ cm^3$$

$$\ell = 2a.$$

Then

$$I_c = 2.6 \times 10^{-24}\ N_o\ cm^{-2} sec^{-1}$$

$$F_c = 2.3 \times 10^{-21}\ N_o\ cm^{-2}$$

$$\frac{\omega}{4\pi} = \frac{2\pi a^2}{4\pi (8\ R_s)^2} = 3.1 \times 10^{-4}$$

$$P'(I_c) = 5 \times 10^{-3}\ (0.55\ R_Z - 2.2)\ N_o^{-0.15}$$

The probability of encountering any flux or fluence levels due to the Probe passing through a bubble-shaped transient is also plotted in Figures 7 and 8 for a year in which the sunspot number is 200. The ratio of the probability of encountering a given flux or fluence due to an immediate escape event to the probability of encountering the same flux or fluence due to a bubble-shaped coronal transient is $P'(I_a)/P'(I_c) = 1/3$. The probability of encountering a rope shaped coronal transient is negligibly small (it is below the bottoms of Figures 7 and 8).

IV. ELECTRONS

A. OBSERVATIONS

To a first approximation, the distribution of the number of electrons at the Sun can be deduced from the distribution of protons calculated from the parameters described above, at least for high intensity events, which are the main concern of this study. This approximation is based on two results:

1a) From Equation (11), it follows that the characteristic source density spectrum (i.e., the number of particles per unit energy and volume) for protons between 20-80 MeV is of the form

$$\delta_p(E) \propto \left(\frac{E}{E_o}\right)^{-3.2 \pm 0.5}$$

and may be assumed to be of the same form down to 10 MeV. At even lower energy, the spectrum may be the same or flatter.

1b) The characteristic density spectrum for electrons had been reported as

$$\delta_e(E) \propto \left(\frac{E}{E_o}\right)^{-3 \pm 0.2}$$ between 3 and 12 MeV (Simnett, 1972)

and $$\delta_e(E) \propto \left(\frac{E}{E_o}\right)^{-3.5}$$ between 12 and 45 MeV (Datlowe, 1971).

Below 3 MeV, a number of observed spectra seem to fit a power low in energy with spectral index 2 to 4 (Lin 1974).

2) The ratio between the 0.2-1.1 MeV electron maximum intensity and the 10 MeV proton maximum intensity was found to be constant for 80% of the events observed at positions well connected to flare regions and with peak intensity > 5×10^{-2} protons/cm^2-sec-sr-MeV (which corresponds approximately to peak intensity > 1×10^{-3} proton/cm^2-sec-sr-MeV for 40 MeV proton events). This relation was first observed qualitatively on a comparison between the maximum intensities of 10 MeV protons and 0.5-1.1 MeV electrons for 42 events detected by the GSFC cosmic ray experiment on the Earth orbiting satellites IMP 4 and IMP 5 from May 1967 to October 1972

(Figure 9). A further comparison using the 0.2-1 MeV maximum electron intensity from the Caltech cosmic ray experiment on IMP 7 versus the 10 MeV maximum proton intensity from the GSFC cosmic ray telescopes on IMP 7 for events detected between October 1972 and September 1974 (Figure 10) confirms the previous result and gives an absolute value for the constant between the intensity of 0.2-1 MeV electrons (mean energy = 0.4 MeV) and 10 MeV protons:

$$\frac{J_e \text{ Max } (0.4 \text{ MeV})}{J_p \text{ Max } (10 \text{ MeV})} \simeq 100 \tag{19}$$

Assuming a spectral index of 3 for electrons above 0.2 MeV, the ratio at constant energy can be represented by:

$$\frac{J_e}{J_p} \simeq 10^{-2} E^{-0.3} \qquad (E \text{ in MeV})$$

However, this is an average value and one should realize that there are fluctuations in the spectrum.

B. MAXIMUM PROBABLE ELECTRON FLUX AND FLUENCE

The range of electron energies of interest is $\geq$ 500 keV. When the spectral shapes $E^{-2.7}$ for protons and $E^{-3.0}$ for electrons are combined with Equation (19) above, we find

$$J_e(0.5 \text{ MeV}) = \left(\frac{0.4}{0.5}\right)^{3.0} \left(\frac{20}{10}\right)^{2.7} 10^2 \, J_p(20 \text{ MeV}) = 333 \, J_p(20 \text{ MeV})$$

Integration over energy gives

$$I_e(\geq 0.5 \text{ MeV}) = \int_{0.5}^{\infty} J_e(0.5 \text{ MeV}) \, (E/0.5)^{-3} \, dE = J_e(0.5 \text{ MeV})/4$$

and

$$I_p(\geq 20 \text{ MeV}) = \int_{20}^{\infty} J_p(20 \text{ MeV}) \, (E/20)^{-2.7} \, dE = 12 \, J_p(20 \text{ MeV})$$

Thus,

$$I_e(\geq 0.5 \text{ MeV}) = \frac{333}{4 \times 12} I_p(\geq 20 \text{ MeV}) = 7\, I_p(\geq 20 \text{ MeV}). \qquad (20)$$

By analogy with Equation (7) in Section IIIB, we find that the maximum probability of encountering a given flux I of $\geq$ 500 keV electrons at 4 R_s is

$$P_{max}(I_e) = \frac{2 \times 10^5}{I_e}$$

where I_e is in units of electrons/cm^2-s. Again, as an example, there is a maximum of a 1% chance of encountering an electron flux of 2×10^7 $cm^{-2}s^{-1}$, or a maximum probability of 1% of encountering a total fluence of 10^{12} energetic electrons/cm^2 during the 16 hour perihelion passage.

C. MOST LIKELY ELECTRON FLUXES AND FLUENCES

The proton probability calculations in Section IIIC can be carried over directly for electrons if we use the result of Equation (20) and let N_o(e's $\geq$ 0.5 MeV) = 7 N_o(p's $\geq$ 20 MeV). Thus Figures 7 and 8 can be applied to energetic electrons by multiplying the flux and fluence scales by a factor of 7.

V. SOLAR NEUTRON FLUXES AND FLUENCES

The estimation of the solar flare neutron flux and fluence near the Sun is difficult due to the fact that a neutron flux of solar origin has not yet been unambiguously detected. This is understandable, since all experimental attempts to identify a solar neutron flux have been made in Earth satellites or balloons, where two physical constraints make detection of solar neutrons an extremely difficult problem. First, the approximately 12-minute half-life of neutrons reduces greatly the flux of low energy neutrons which could survive to 1 AU. Secondly, local neutron background generated in the spacecraft--mainly the cosmic radiation--have placed severe limits on the sensitivity for detection. Indeed, only upper limits on neutron fluxes have been reported (Lockwood et al., 1973; Kirsch, 1973). Figure 11 illustrates the effect of the decay of neutrons of selected energies as a function of radial distance. The measurement of this dependence has been proposed as a means to identify solar neutrons and to separate the solar from background neutron fluxes (Anglin et al., 1972). Two components of solar neutron fluxes are expected to be present, namely:

A. Quasi-steady solar neutron production which, though primarily from extended areas of solar activity, may also exist at lower levels and energies over the local photosphere (mainly 10 keV to 1 MeV neutrons), and

B. Impulsive neutron production from solar flares associated with collisions between accelerated charged particles and the chromospheric and coronal material (mainly 1-100 MeV neutrons).

Because neutrons have long mean free paths for propagation through spacecraft materials and can produce interstitial damage in semiconductor devices, we must decide whether neutrons could represent a significant hazard for the proposed Solar Probe missions. In this Section, we estimate the neutron flux and fluence possible from solar flare events, which undoubtedly have higher intensities and energies than do neutrons from quasi-steady production mechanisms (see A above).

Two approaches to estimating neutron fluxes from flares are possible:

1) The upper limit for production of secondary nuclei produced in flares could be used for large flares (H^1, H^2, H^3, He^3, etc.), or

2) evidence from nuclear gamma rays could be invoked. In this note we follow the latter approach which was worked out in principle for the large flare of August 4, 1972, by Ramaty, Kozlovsky and Lingenfelter (1975; referred to as RKL). They calculated both:

   a) the neutron production spectrum, and

   b) the yield of gamma rays due to neutron capture on protons (2.2 MeV gamma ray line) and excited states of nuclei in the solar atmosphere (e.g., the 4.4 MeV carbon line),

   assuming unit values for the "emission measure" for the flare, that is, the product of the density in the interaction region and the intensity of high energy primary protons. The observations by Chupp, Forrest, and Suri (1972) of the gamma ray flux provide the normalization factors necessary to calculate the expected neutron flux for the August 4, 1972, solar flare.

For the calculation of the neutron flux as a function of distance from the Sun, a neutron emission flux is used which is of the form:

$$q\ (E_n) = \begin{cases} q_o \text{ for } E_n < 30 \text{ MeV} \\ q_o \left(\frac{E_n}{30}\right)^{-2} \text{ for } E_n > 30 \text{ MeV} \end{cases}$$

i.e., independent of energy up to 30 MeV and then falling as E^{-2} (after Figure 7 of RKL).

For the 4 August 1972 solar flare the normalization factor q_o is:

$$q_o = q\ (E=0) \cdot n_H N_p\ (> 30 \text{ MeV}) \cdot P_E = 6 \times 10^{25} \text{ neutrons/MeV sec}$$

where

$q\ (E=0)$ is the neutron production rate for unit emission measure, taken to be 2×10^{-18} MeV^{-1} sec^{-1}, (after Figure 7 of RKL)

$n_H N_p$ (> 30 MeV) is the emission measure, calculated by RKL on the basis of the gamma-ray observations to be $\sim 5 \times 10^{43}$ for the solar flare of August 4, 1972, and

P_E is the probability of neutron escape from the production region, taken to be 0.6 independent of neutron energy (Wang and Ramaty, 1974).

These results were taken from the RKL model calculation for the thin target model with a power law primary spectrum but the results are not changed significantly (factor of ~ 5) for other models calculated by RKL.

The solar neutron flux as a function of neutron energy and distance from the Sun, is then calculated from

$$J\ (E_n,R) \ = \ q\ (E_n) \cdot Ps\ (E_n,R) \cdot R^{-2}$$

where

Ps (E_n,R) is the probability that a neutron of energy E_n will survive to travel a distance R. This function, divided by R^2 is plotted in Figure 11 for neutron energies of 10 keV, 1 MeV, and 100 MeV.

In Figure 12 is plotted our calculation of the expected neutron energy spectrum for the August 4, 1972, flare at distances from the flare site of 5, 10, and 20 solar radii and 0.2, 0.5, and 1.0 AU. In Figures 13 and 14, the integral neutron flux (integrated over neutron energy to 10^3 MeV) is plotted for R = 0.01 to 1.0 AU (Figure 13) and R = 2 to 50 solar radii (Figure 14). (The major contributions to this integral are from neutrons of energy 1 MeV to 100 MeV.)

The extrapolation of these results to flares other than the 4 August 1972 flare is, at best, tenuous. With neither neutron nor gamma ray observations, the only other normalization factor available is the high energy proton flux.

Of 25 solar flares defined as "major" by King (1974) which occurred during solar cycle 20 from 1966 to 1972, the August 4, 1972, flare was the largest. Total fluences of protons with energy above 10 MeV ranged

from ∿10% to 0.1% of the August flare fluence. Presumably the expected neutron flux may be scaled from flare to flare in proportion to the observed proton fluence. Thus one may naively expect an average "major" flare to contribute a neutron flux of a few percent of the values calculated here. Finally, due to the fact that the neutron pulse from a flare is so short (on the order of an hour) any observer will either see the flare and be subject to the full neutron fluence or will be on the wrong side of the Sun and see nothing. Assuming an isotropic neutron angular emission distribution, any observer will see ∿ half of all neutron events.

In summary, for the spacecraft on a trajectory which passes within 10 R_s of the Sun, the neutron fluence for a flare on the "visible" side of the Sun of the magnitude of the August 4, 1972, event, and with neutron emission occurring for $\sim 10^3$ sec, will be $\sim 10^6 - 10^7$ neutrons/cm^2 in the energy range 1-100 MeV.

VI. CONCLUSIONS

In the present concept of the Solar Probe mission, an eccentric, low perihelion orbit is attained by a Jupiter gravity-assist maneuver. The near-Jupiter trajectory is similar to that for the Solar Polar mission for which the predicted energetic particle populations are given in Table 3. For ease of the implementation of the Solar Probe mission, we require that there be no more than a 1% chance that the peak flux and fluence of energetic particles near the Sun exceed that of the Jupiter flyby.

TABLE 3. PREDICTED ENERGETIC PARTICLE ENVIRONMENT FOR JUPITER PHASE OF THE SOLAR POLAR MISSION

Particle	Peak flux, $cm^{-2}s^{-1}$	Fluence (unshielded) cm^{-2}
Protons $\geq$ 20 MeV	10^6	10^{12}
Electrons $\geq$ 0.5 MeV	10^8	10^{14}

From Table 1, we see that the upper limits on energetic solar particles calculated from solar photons are many orders of magnitude above the Jovian values. As noted earlier, in the next few years the quality of the observations may improve to the point that actual values can be calculated rather than upper limits.

From Equation (7), there is a maximum probability of 1% of encountering a flux of 3×10^6 energetic protons $cm^{-2}s^{-1}$ during the solar flyby, which is close to the peak level during the Jupiter flyby.

At 2×10^{11} cm^{-2}, the 1% maximum probable proton fluence is below the Jupiter level. Since the spacecraft may be at the Sun close to the time of solar activity maximum, we use the bubble transient, $R_Z = 200$ line in Figure 7 to predict that there is only a 0.2% chance of a flux as high as 10^6 $cm^{-2}s^{-1}$ during the solar flyby. From Figure 8 we see that there is also very little chance of exceeding the proton fluence of 10^{12} cm^{-2} predicted for the Jupiter phase of the mission.

Note from Table 3 that at Jupiter $I_e(\geq 0.5$ MeV$)/I_p(\geq 20$ MeV$) = 10^2$, whereas the solar particle energy spectra yield a ratio of only 7 (see Equation (20)). Thus, energetic electrons should not be a problem either.

For the Solar Polar mission, the predicted flux of 1 - 3 MeV neutrons from the radioisotope thermal generator is 80 $cm^{-2}s^{-1}$. From Figure 12, we see that for the very large flare of 4 August, 1972, the neutron flux in this energy range was perhaps 1400 $cm^{-2}s^{-1}$ at 5 R_s. Thus, in this energy range, we expect the solar neutron flux to exceed the background level from the power supply only a few hours a year. Thus, although it is unlikely that solar neutrons would be hazardous to the health of the spacecraft, there is a severe problem in limiting the neutron flux from the power supply to levels which allow solar neutrons to be measured.

One might conclude that flying by the Sun at 4 R_s is less hazardous than flying by Jupiter. A solar flyby is not without risks, however. First, we could be unlucky and meet an extremely rare, but large flare. About one flare per ten or twenty years may emit on the order of 10^{36} energetic protons, which, according to Equations (15) and (16), would yield fluxes and fluences at the Solar Probe of 6×10^7 $cm^{-2}s^{-1}$ and 10^{12} cm^{-2}, respectively. Such a flux would far exceed the peak flux of the Jupiter encounter; the fluence would be approximately the same. Second, some of the assumptions made in Sections III and IV may not be correct. For example, we assumed that particles travel from the Sun to 1 AU with no change of energy. If there were some mechanism which causes an adiabatic energy loss near the Sun, the flux and fluence at a given energy could be very much higher near the Sun than we have calculated. Third, although low energy particles ($\sim$ 1 MeV) are not a severe hazard for the internal components of the spacecraft, they may be a serious concern for surface elements such as thermal control surfaces and sensor surfaces (optical, etc.). An important difference between low and high energy particles from solar events is that at low energies the events may last for many days with very long injection times. Therefore, the probable flux of low energy particles may not simply scale as the observed energy spectrum near the peaks of events.

Finally, although, with proper shielding, the Jupiter encounter radiation levels may not be physically damaging to the equipment, they may very well be a strong source of interference. For example, special precautions may be necessary to prevent energetic particles from causing unacceptable background counting rates or currents in the plasma and imaging instruments.

In summary, although we must continue to improve our models over the next few years, a first quick look at the problem indicates that energetic particles are probably not a safety hazard for a 4 R_S flyby of the Sun.

REFERENCES

Anglin, J. D., Dietrich, W. F., and Simpson, J. A., High Energy Phenomena on the Sun, Ramaty, R. and Stone, R. G. (eds.), NASA SP-342, National Aeronautics and Space Administration, Washington, D.C., p. 315, 1972.

Chupp, E. L., Larakase, P. J., and Sarkady, A. A., Phys. Rev., 166, 1299, 1968.

Chupp, E. L., Forrest, D. J., and Suri, A. N., High Energy Phenomena on the Sun, Ramaty, R. and Stone, R. G. (eds.), NASA SP-342, National Aeronautics and Space Administration, Washington, D.C., p. 285, 1972.

Chupp, E. L., Forrest, D. J., Higbie, P. R., Suri, A. N., Tsai, C., and Dunphy, P. P., Nature, 241, 333, 1973.

Datlowe, D., Solar Physics, 17, 436, 1971.

Datlowe, D. W., in Solar Gamma, X- and EUV Radiation, Kane, S. R. (ed.), D. Reidel Publishing Co., Dordrecht-Holland/Boston-USA, p. 191-208, 1974.

Fainberg, J., and Stone, R. G., Space Sci. Rev., 16, 145, 1974.

Gold, R. E., Keath, E. P., Roelof, E. C., and Reinhard, R., Proc. 15th International Cosmic Ray Conference, 5, 125, 1977a.

Gold, R. E., Krimigis, S. M., and Roelof, E. C., Proc. 15th International Cosmic Ray Conf., 5, 119, 1977b.

Gosling, J. T., Hildner, E., MacQueen, R. M., Munro, R. H., Poland, A. I., and Ross, C. L., J. Geophys. Res., 79, 4581, 1974.

Hildner, E., Gosling, J. T., MacQueen, R. M., Munro, R. H., Poland, A. I., and Ross, C. L., Solar Phys., 48, 127, 1978.

Kane, S. R., private communication, 1978.

King, J. H., J. Spacecraft and Rockets, 11, 401, 1974.

Kirsch, E., Solar Phys., 28, 223, 1973.

Lin, R. P., Space Sci. Rev., 16, 189, 1974.

Lin, R. P., and Hudson, H. S., Solar Phys., 50, 153, 1976.

Lockwood, J. A., Ifedili, S. O., and Jenkins, R. W., Solar Phys., 30, 183, 1973.

McDonald, F. B., Fichtel, C. E., and Fisk, L. A., High Energy Particles and Quanta in Astrophysics, McDonald, F. B. and Fichtel, C. E. (eds.), p. 212, 1974.

McDonald, F. B., Teegarden, B. J., Trainor, J. H., von Rosenvinge, T. T., and Webber, W. R., Ap. J., 203, L149, 1976.

McKibben, R. B., J. Geophys. Res., 77, 3957, 1972.

Newkirk, G., Ann. Rev. Astron. Astrophys., 5, 213, 1967.

Pneuman, G., Solar Phys., 4, 578, 1968.

Pneuman, G., Solar Phys., 28, 247, 1973.

Ramaty, R., Kozlovsky, B., and Lingenfelter, R. E., Space Sci. Rev., 18, 341, 1975.

Reedy, R. C., Proceedings of the Lunar Science Conference, 8, 825, 1977.

Roelof, E. C., Gold, R. E., Krimigis, S. M., Krieger, A. S., Nolte, J. T., and McIntosh, P. S., Proc. 14th International Cosmic Ray Conf., 5, 1704, 1975.

Shea, M. A., and Smart, D. F., 13th Intl. Conf. Cosmic Ray, Denver, 2, 1548, 1973.

Simnett, G. M., Solar Phys., 22, 189, 1972.

Tousey, R., Howard, R. A., and Koomen, M. J., Bull. Amer. Astron. Soc., 6, 295, 1974.

Van Hollebeke, M. A. I., Ma Sung, L. S., and McDonald, F. B., Solar Phys., 41, 189, 1975.

Van Hollebeke, M. A. I., McDonald, F. B., Trainor, J. H., and von Rosenvinge, T. T., GSFC/NASA TM 78040 (to be published in JGR), 1978.

Wang, H. T., and Ramaty, R., Solar Phys., 36, 129, 1974.

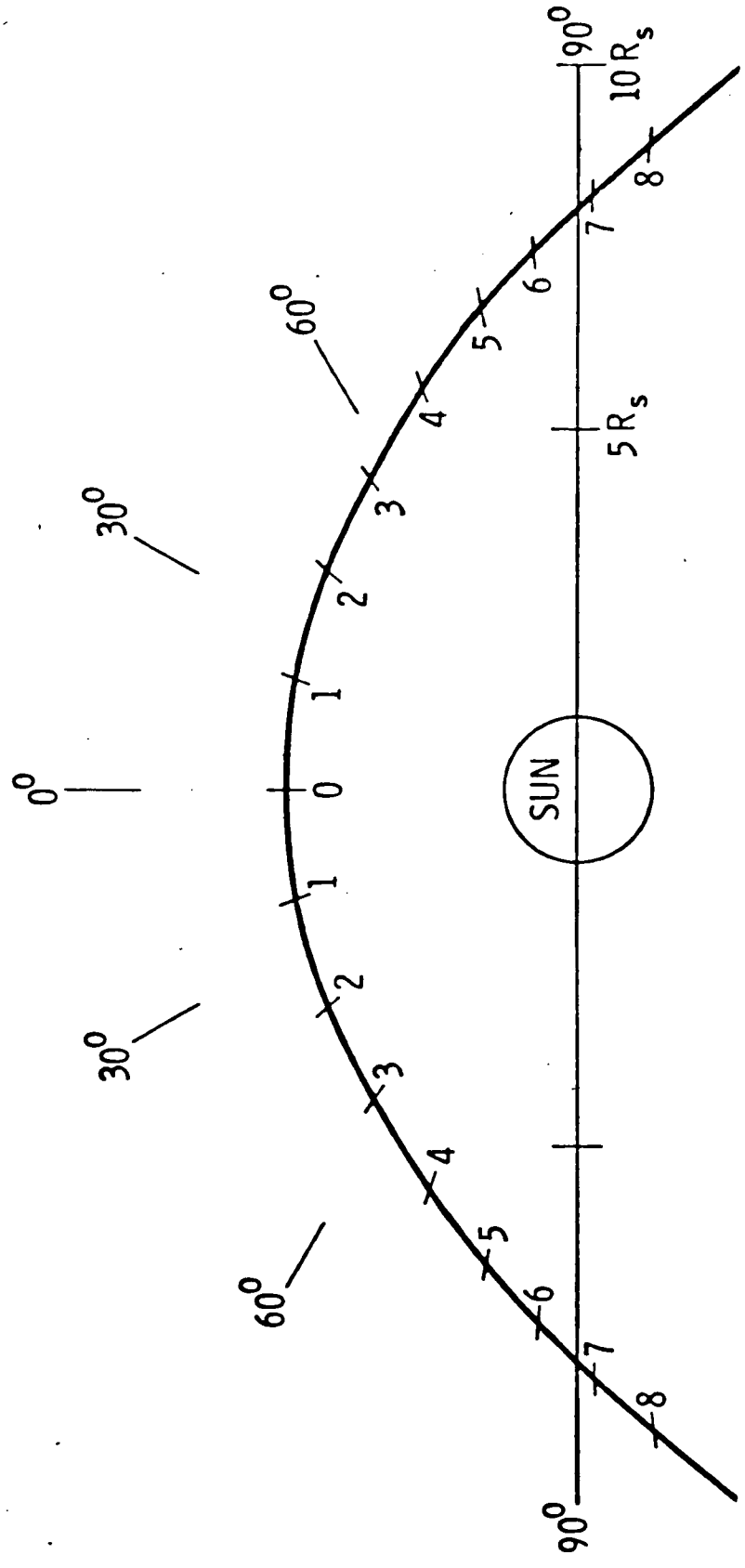

Figure 1. The near solar portion of the planned Solar Probe trajectory shows angles, distance (in solar radii) and times (in hours) from closest approach.

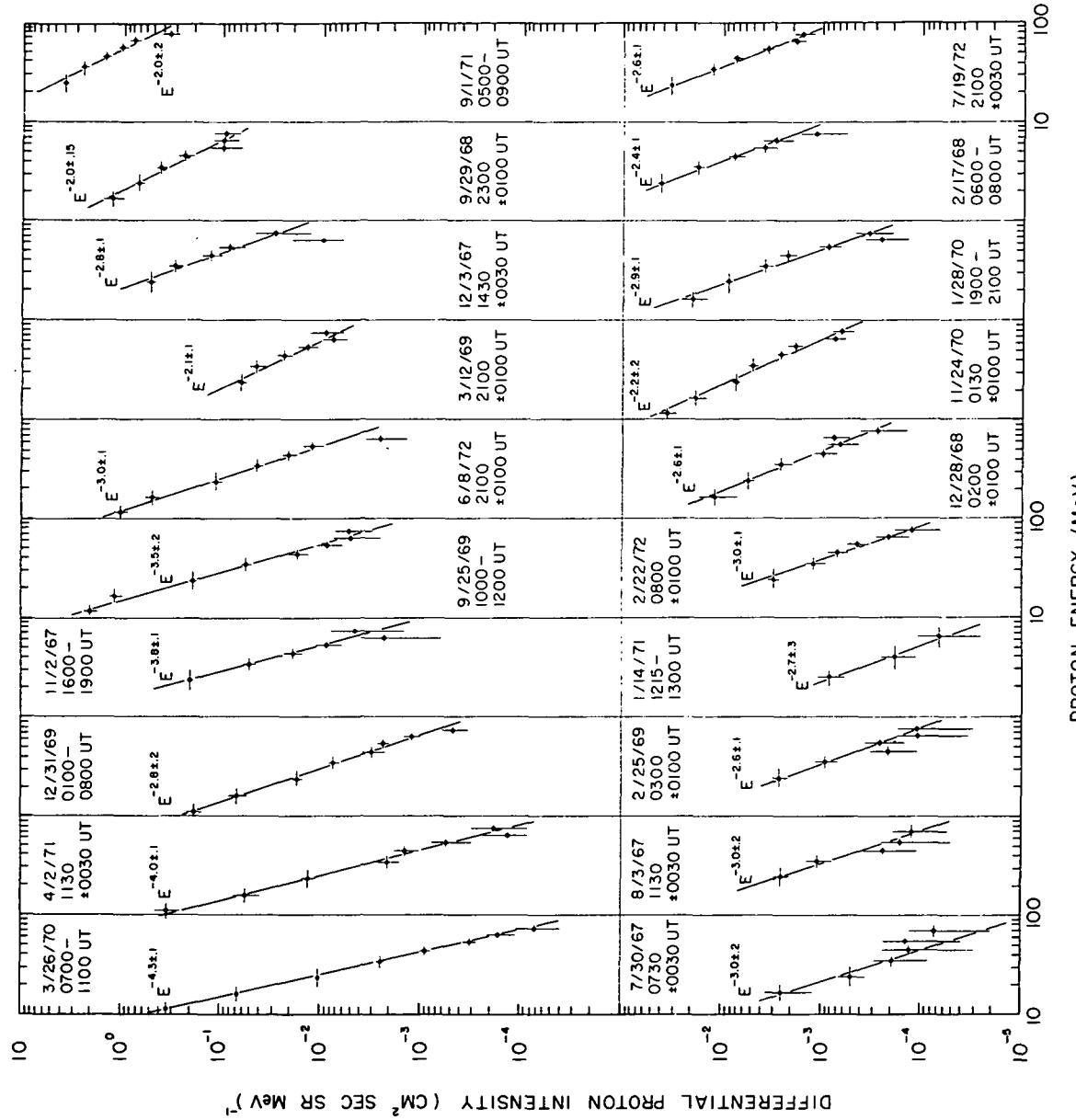

Figure 2. Representative samples of proton spectra.

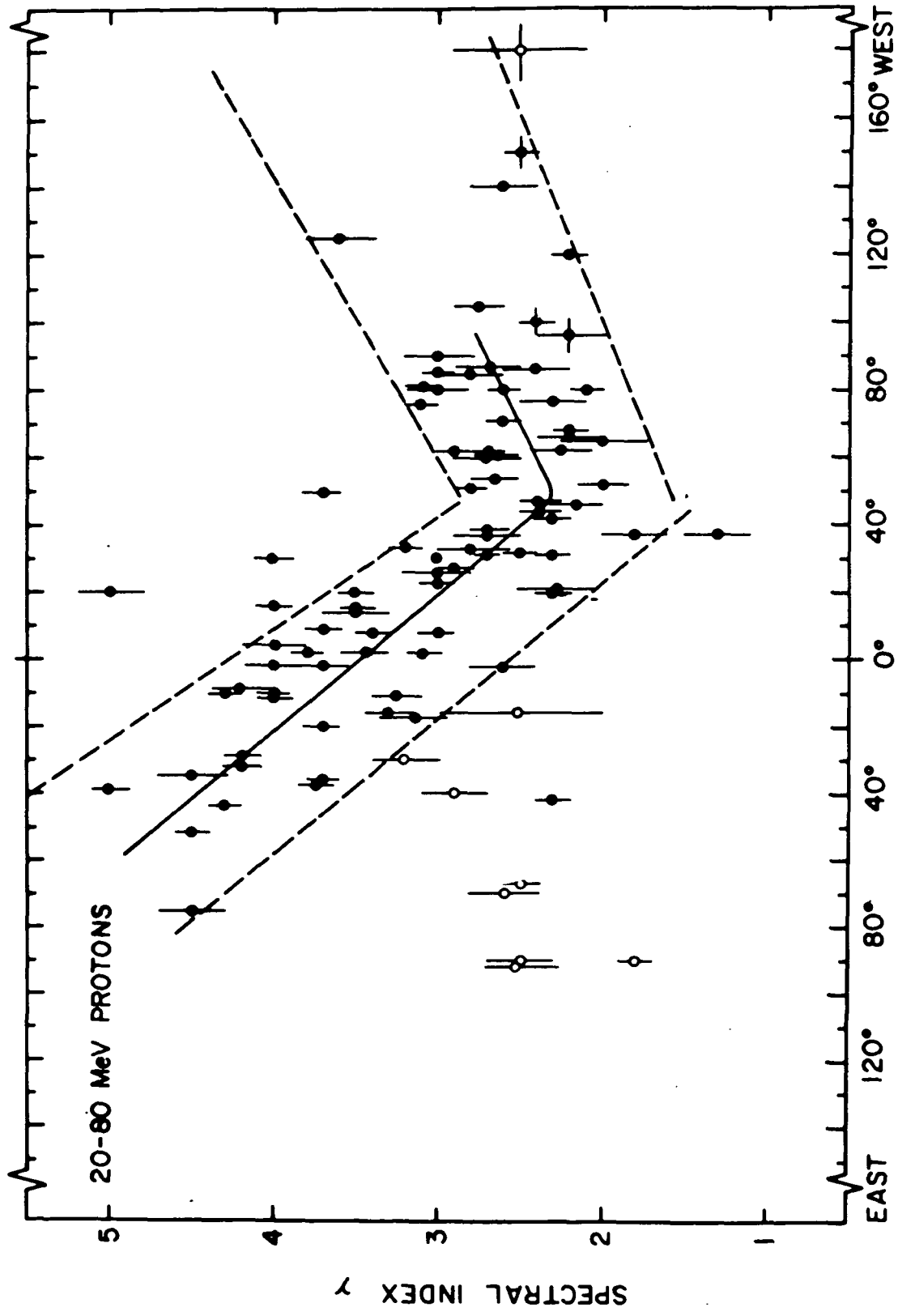

Figure 3. Measured spectral index γ as a function of heliolongitude.

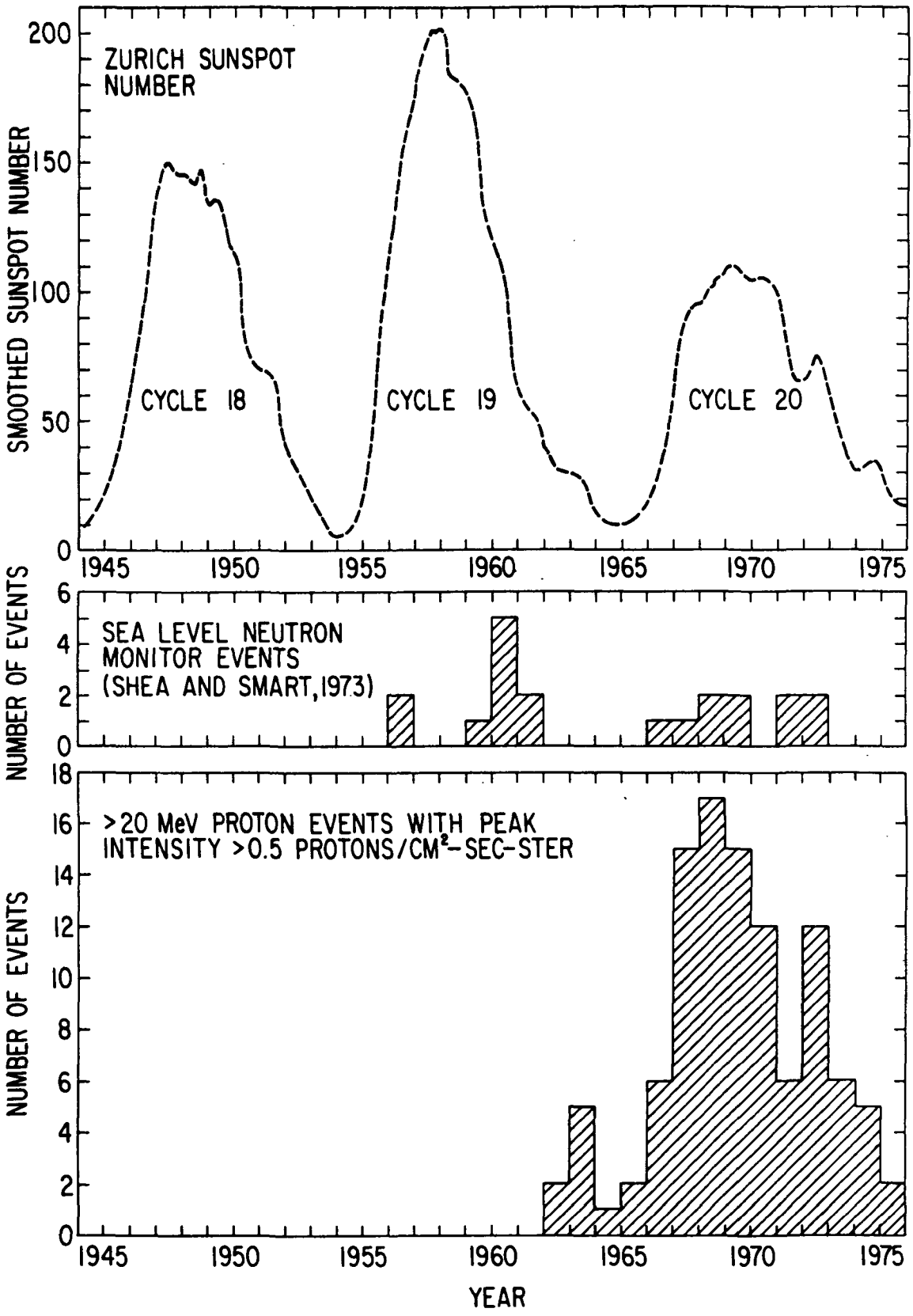

Figure 4. Time histories of the number of proton events, the number of neutron events, and the sunspot number.

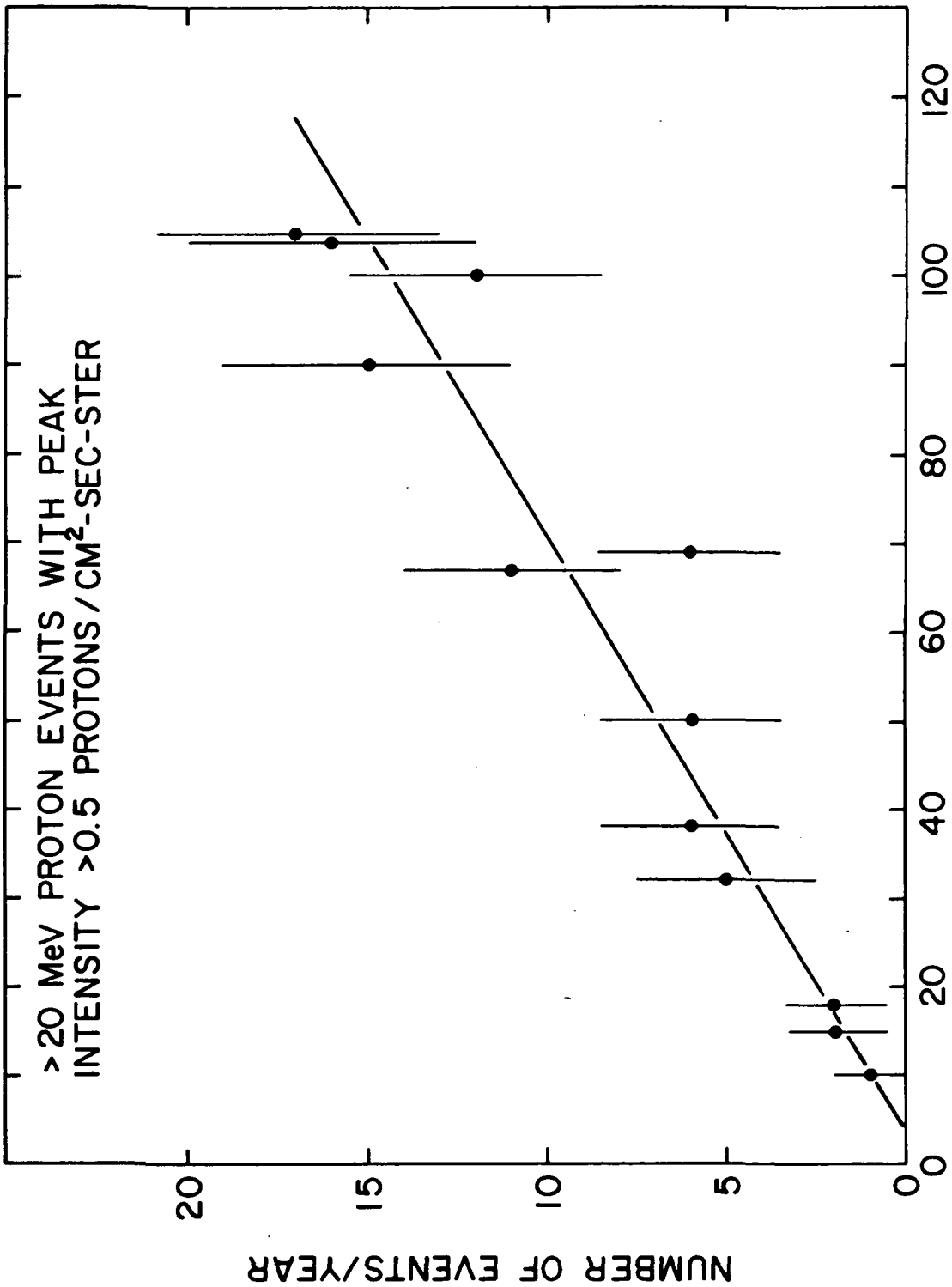

Figure 5. Sunspot number plotted versus proton event frequency.

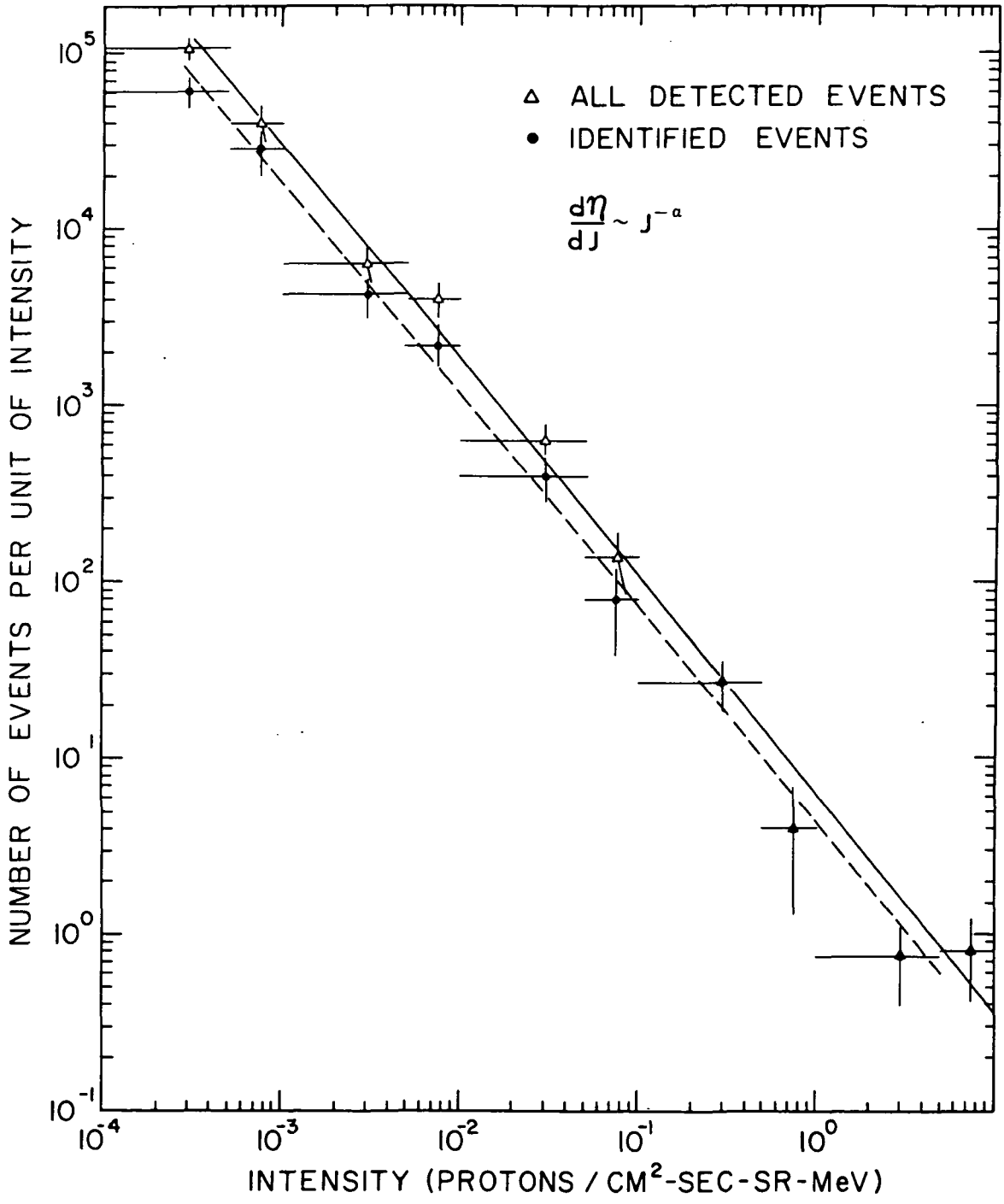

Figure 6. The relation of the number of events per unit intensity as a function of intensity for data from 1967 to 1972.

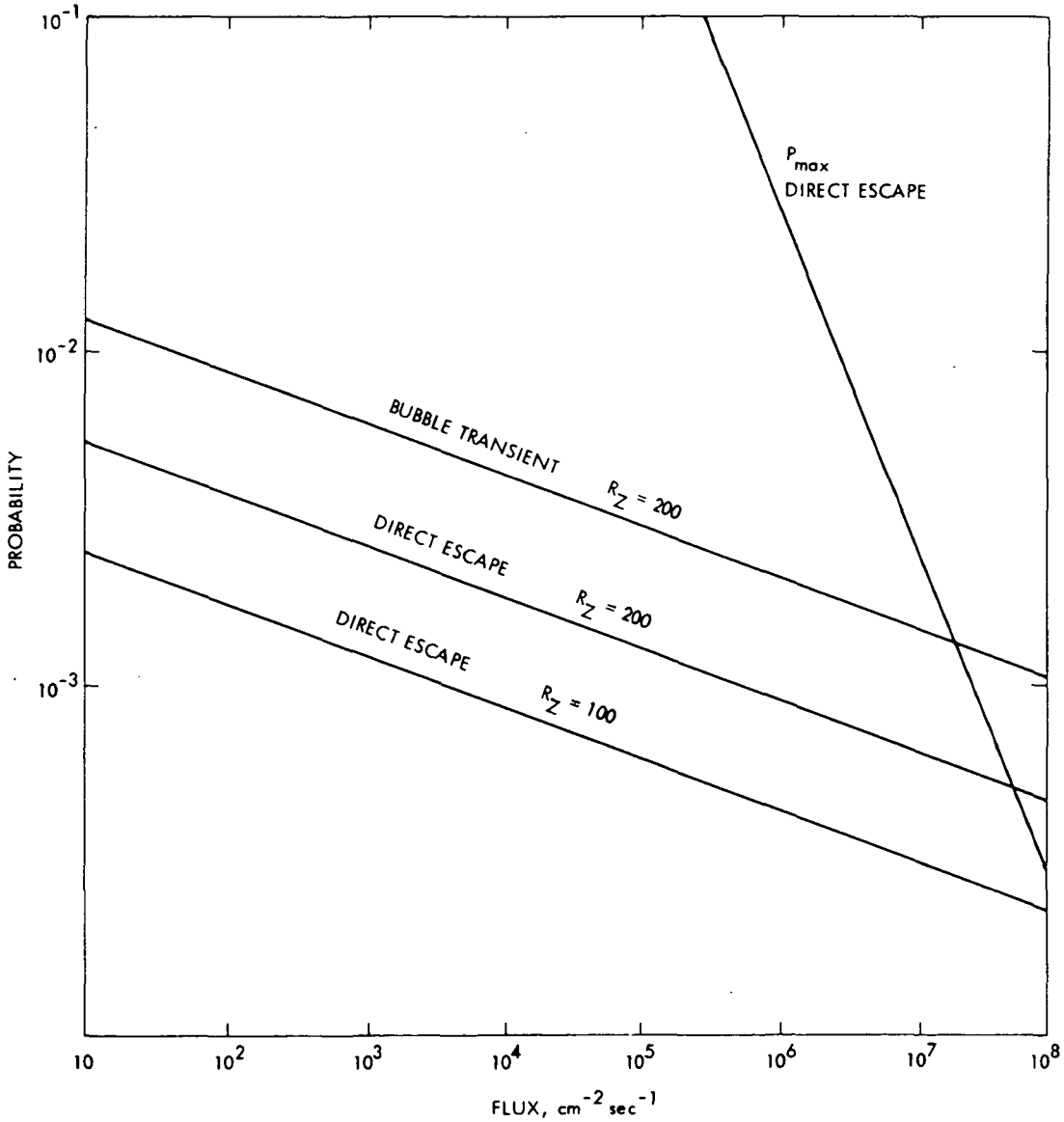

Figure 7. The probabilities of the spacecraft encountering fluxes of given levels for sunspot numbers of 100 and 200 per year and for immediate escape and bubble transients. The steepest line is the maximum probability as defined in Section IIIB.

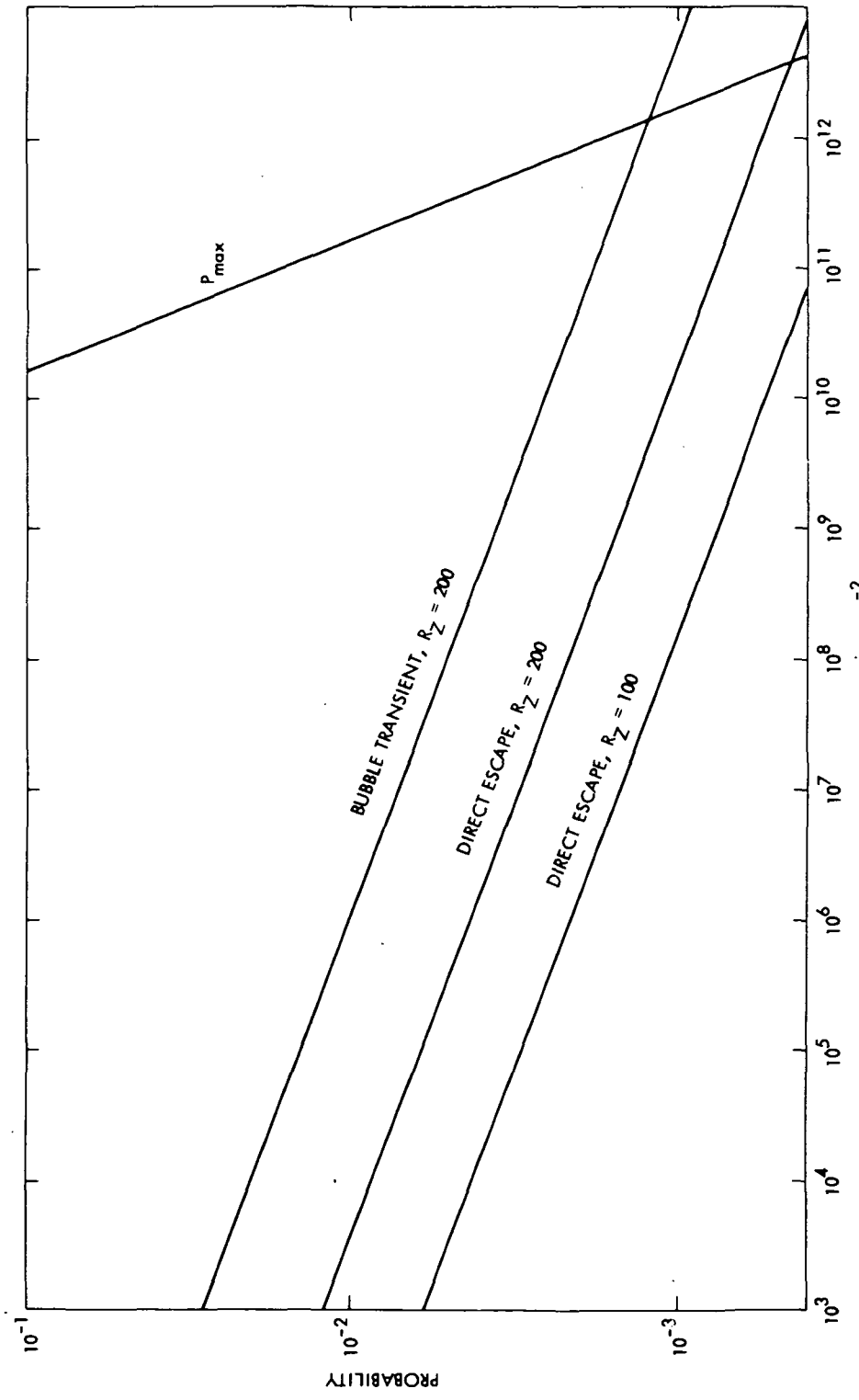

Figure 8. The probabilities of the spacecraft encountering fluences of given levels for sunspot numbers of 100 and 200 per year and for immediate escape and bubble transients. The steepest line is the maximum probability as defined in Section IIIB.

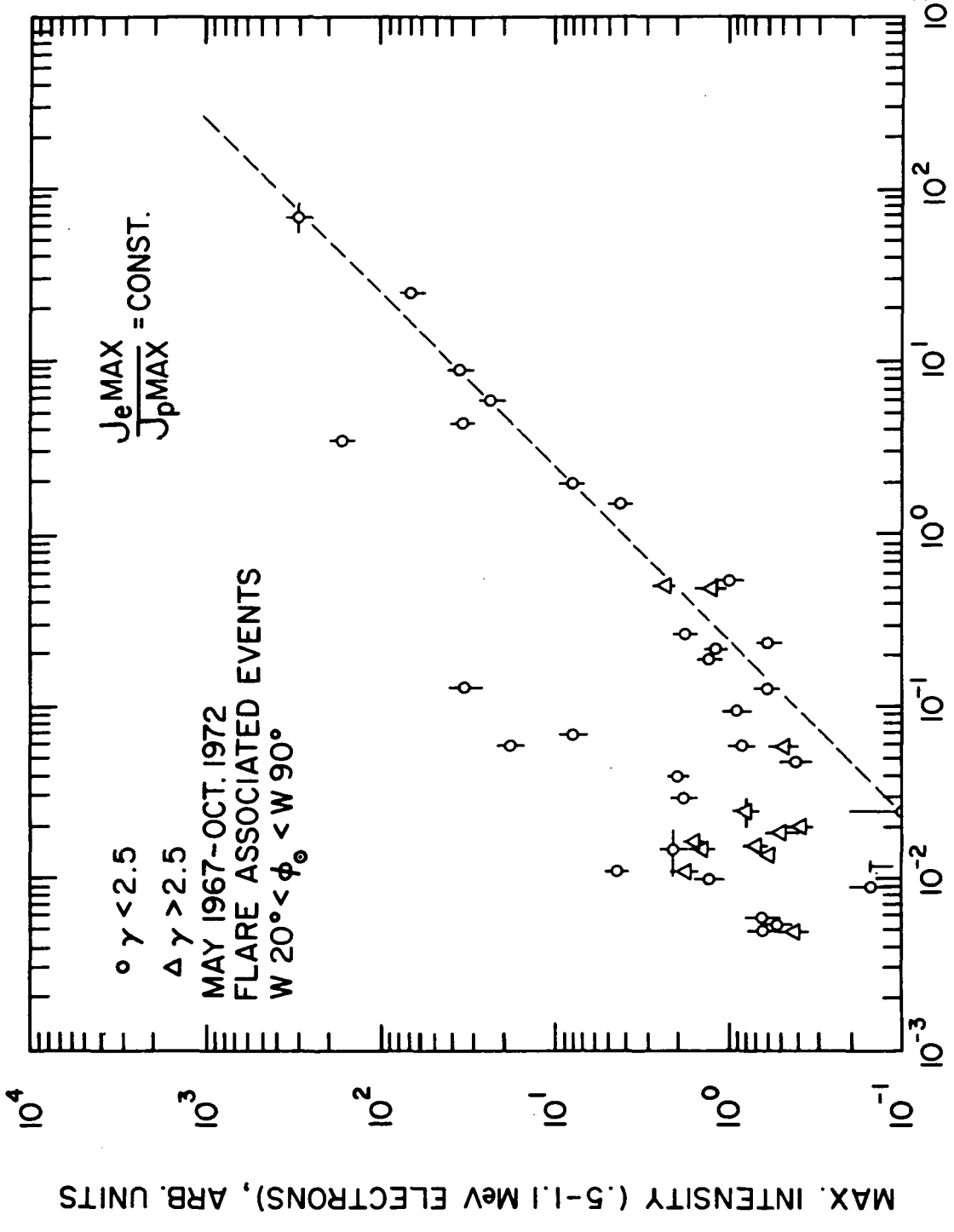

Figure 9. Maximum intensities for electron and proton events are plotted to show a constant ratio. These data are from the GSFC group from 1967 to 1972.

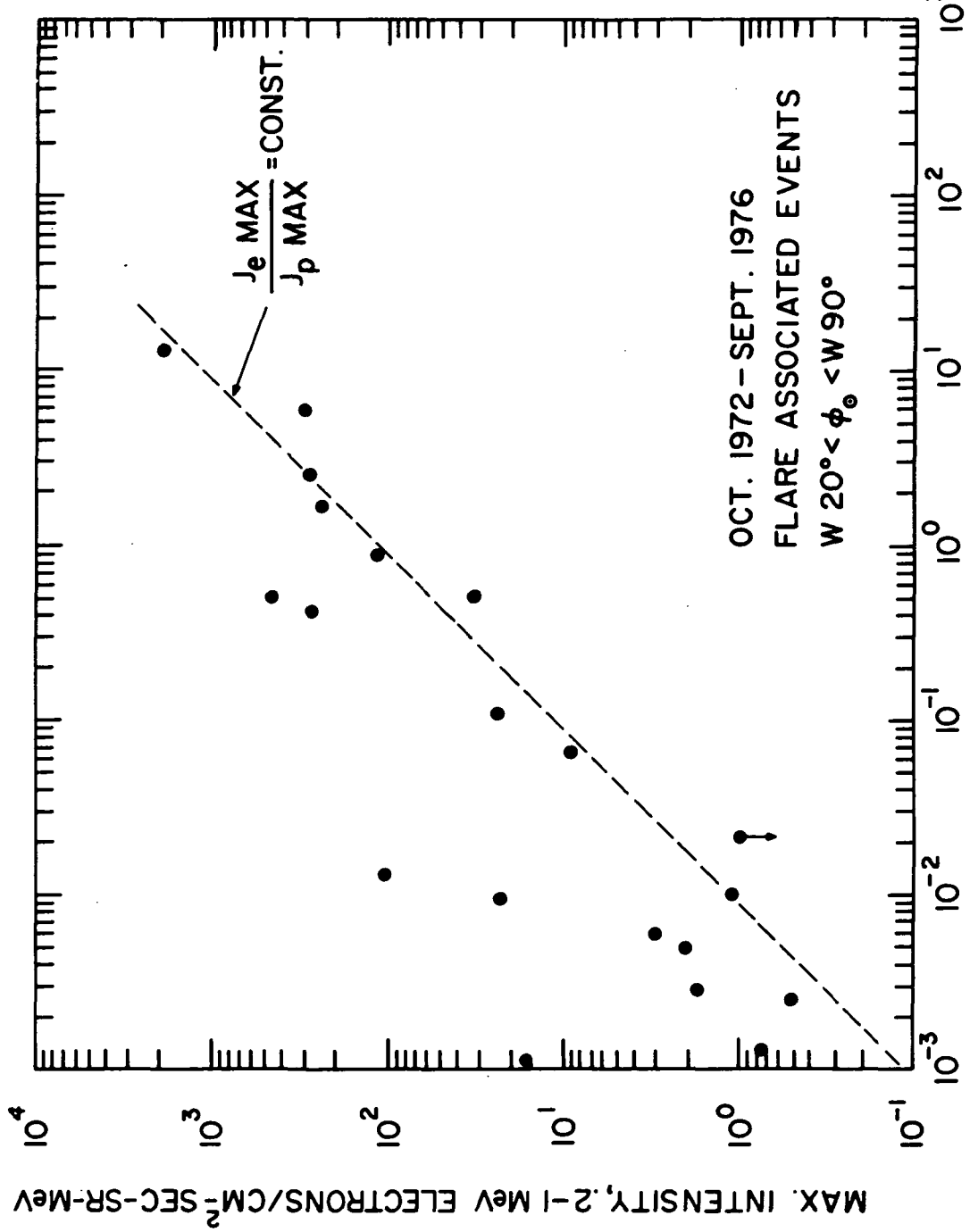

Figure 10. Data from the Caltech group from 1972 to 1974 show similar results to those in Figure 9.

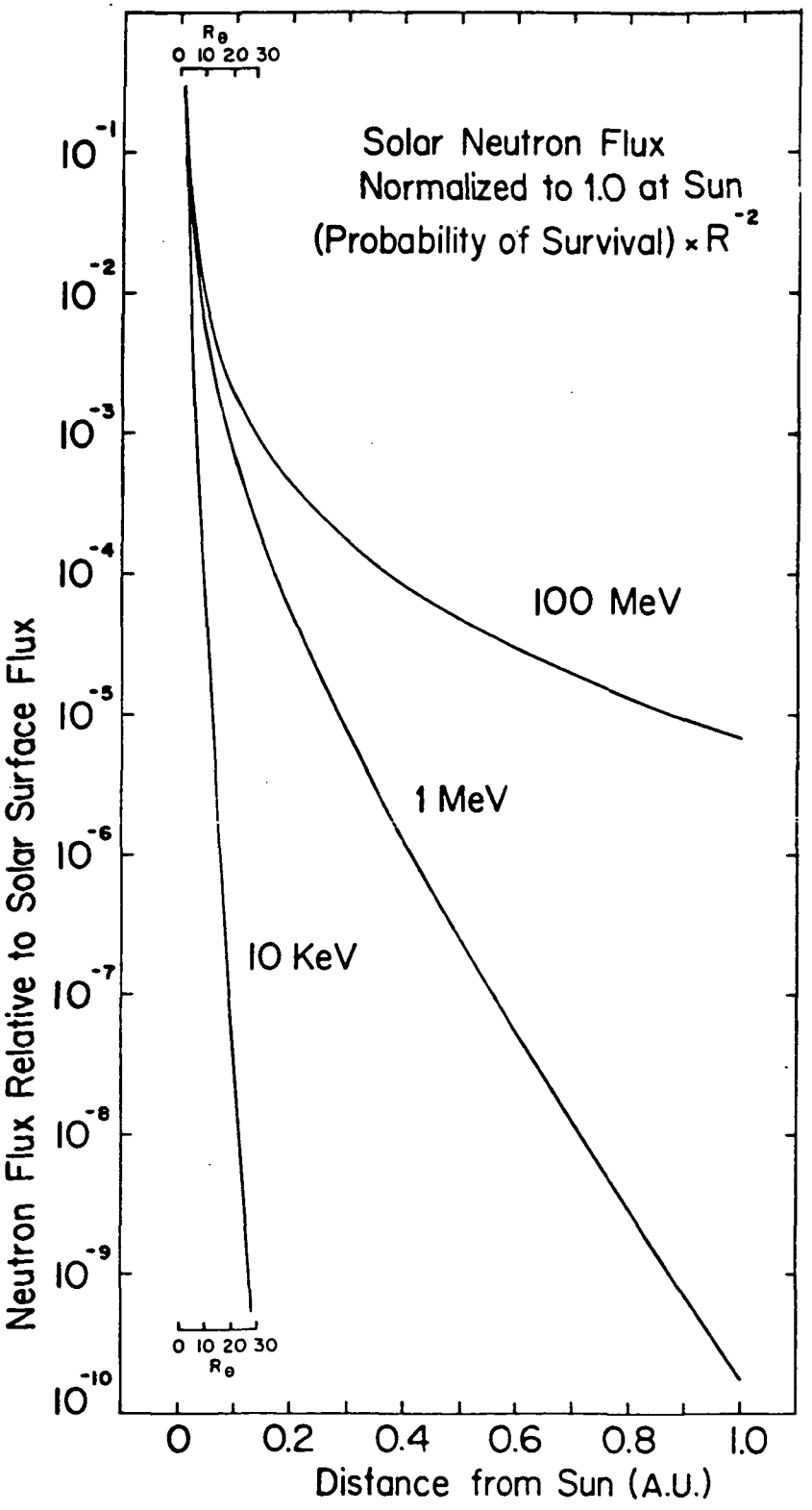

Figure 11. The dependence of the normalized neutron flux as a function of radial distance from the Sun for three decades of neutron energies.

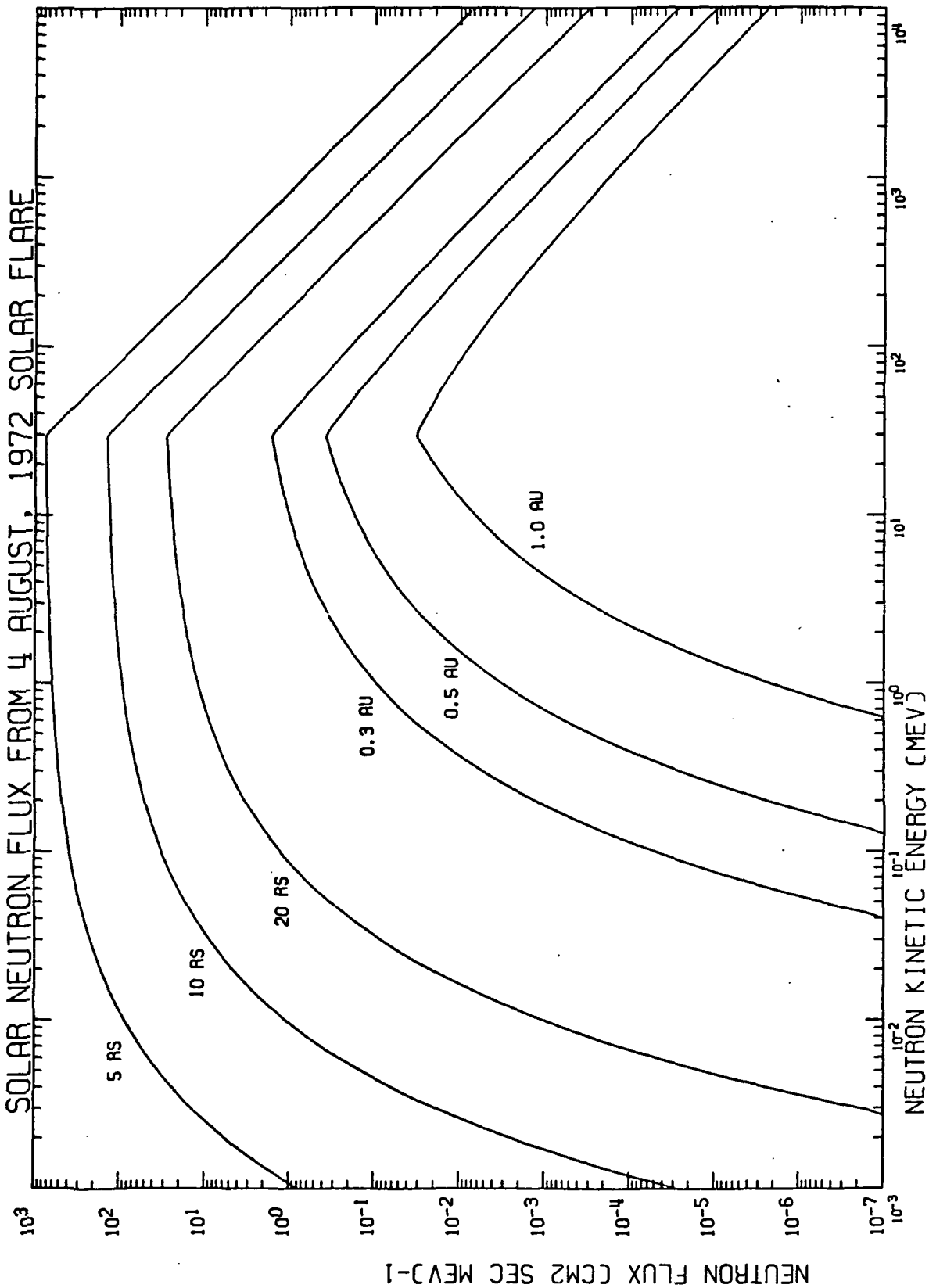

Figure 12. Calculated values of neutron flux versus kinetic energy for various distances from the site of the August 4, 1972, flare.

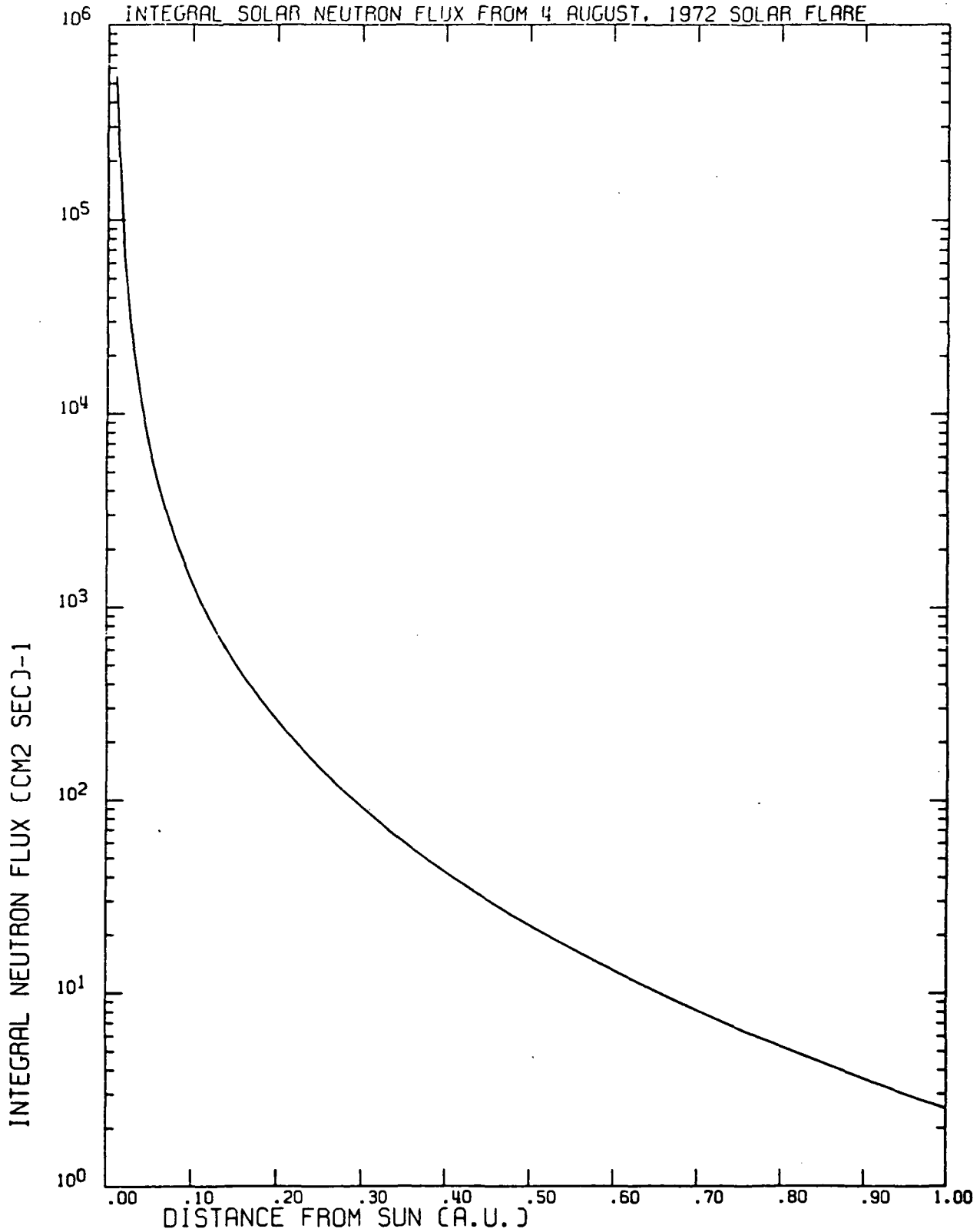

Figure 13. The neutron flux density integrated over neutron energy to 1000 MeV versus solar distance.

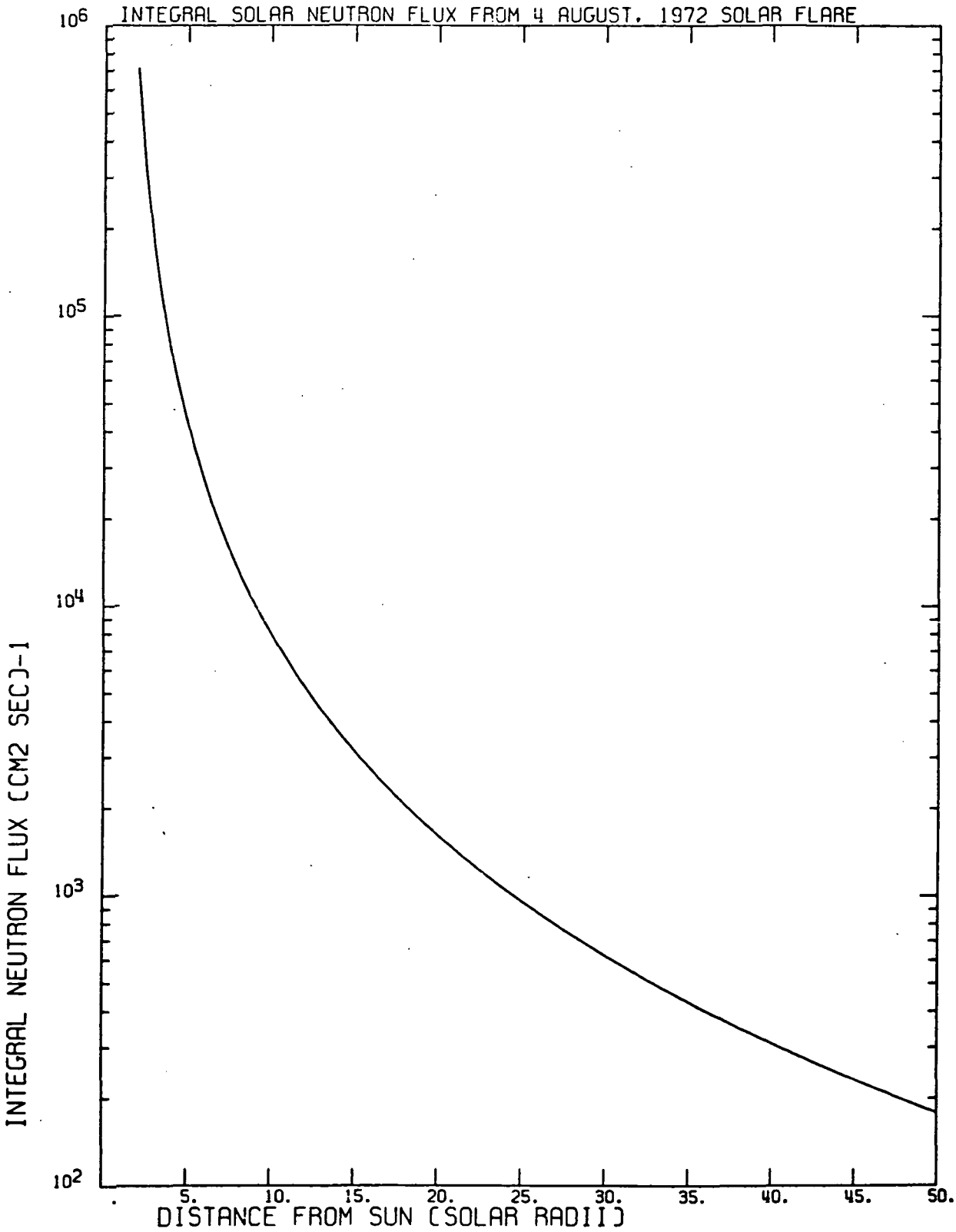

Figure 14. An expanded view of Figure 13 close to the Sun.

NASA—JPL—Coml., L.A., Calif.